(12) INTERNATIONAL APPLICATION PUBLISHED UNDER THE PATENT COOPERATION TREATY (PCT)

(19) World Intellectual Property Organization
International Bureau

(43) International Publication Date
20 December 2012 (20.12.2012)

WIPO | PCT

(10) International Publication Number
WO 2012/172084 A2

(51) International Patent Classification:
G02B 1/04 (2006.01)

(21) International Application Number:
PCT/EP2012/061513

(22) International Filing Date:
15 June 2012 (15.06.2012)

(25) Filing Language: English

(26) Publication Language: English

(30) Priority Data:
1110018.7 15 June 2011 (15.06.2011) GB

(71) Applicant *(for all designated States except US)*: **DEUTSCHES KUNSTSTOFF-INSTITUT** [DE/DE]; Schlossgartenstr. 6, 64289 Darmstadt (DE).

(72) Inventors; and

(75) Inventors/Applicants *(for US only)*: **HELLMANN, Götz Peter** [DE/DE]; Deutsches Kunststoff-Institut, Schlossgartenstr. 6, 64289 Darmstadt (DE). **SPAHN, Peter Wolfgang Andreas** [DE/DE]; Spessartstrasse 75, 63457 Hanau (DE).

(74) Agents: **NAYLOR, Matthew** et al.; Mewburn Ellis LLP, 33 Gutter Lane, London Greater London EC2V 8AS (GB).

(81) Designated States *(unless otherwise indicated, for every kind of national protection available)*: AE, AG, AL, AM, AO, AT, AU, AZ, BA, BB, BG, BH, BR, BW, BY, BZ, CA, CH, CL, CN, CO, CR, CU, CZ, DE, DK, DM, DO, DZ, EC, EE, EG, ES, FI, GB, GD, GE, GH, GM, GT, HN, HR, HU, ID, IL, IN, IS, JP, KE, KG, KM, KN, KP, KR, KZ, LA, LC, LK, LR, LS, LT, LU, LY, MA, MD, ME, MG, MK, MN, MW, MX, MY, MZ, NA, NG, NI, NO, NZ, OM, PE, PG, PH, PL, PT, QA, RO, RS, RU, RW, SC, SD, SE, SG, SK, SL, SM, ST, SV, SY, TH, TJ, TM, TN, TR, TT, TZ, UA, UG, US, UZ, VC, VN, ZA, ZM, ZW.

(84) Designated States *(unless otherwise indicated, for every kind of regional protection available)*: ARIPO (BW, GH, GM, KE, LR, LS, MW, MZ, NA, RW, SD, SL, SZ, TZ, UG, ZM, ZW), Eurasian (AM, AZ, BY, KG, KZ, RU, TJ, TM), European (AL, AT, BE, BG, CH, CY, CZ, DE, DK, EE, ES, FI, FR, GB, GR, HR, HU, IE, IS, IT, LT, LU, LV, MC, MK, MT, NL, NO, PL, PT, RO, RS, SE, SI, SK, SM, TR), OAPI (BF, BJ, CF, CG, CI, CM, GA, GN, GQ, GW, ML, MR, NE, SN, TD, TG).

Published:

— *without international search report and to be republished upon receipt of that report (Rule 48.2(g))*

WO 2012/172084 A2

(54) Title: COMPOSITE OPTICAL MATERIALS EXHIBITING STRUCTURAL COLOUR

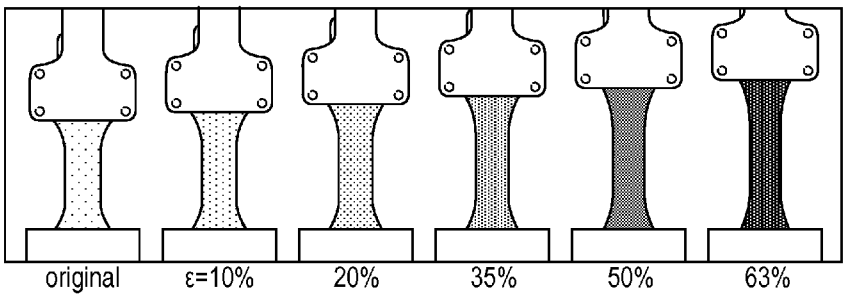

FIG. 1

(57) Abstract: A composite optical material such as a polymer opal is provided having a three dimensional arrangement of core particles distributed in a matrix. The refractive index of the material of the core particles is different to the refractive index of the material of the matrix and the three dimensional arrangement has a periodicity such that, when a surface of the material is illuminated with white light, the composite material exhibits structural colour. The three dimensional periodic arrangement is a reduced symmetry arrangement based on a crystallographic close-packed arrangement but strained therefrom to have reduced symmetry compared to the crystallographic close-packed arrangement. Bragg reflections from planes that would be forbidden in the crystallographic close-packed arrangement are allowed and visible in the reduced symmetry arrangement. This provides a variation in intensity and/or wavelength of structural colour with rotation of the material about an axis perpendicular to the surface when viewed obliquely while the viewing angle remains substantially constant. Also disclosed are methods for the manufacture of such material.

COMPOSITE OPTICAL MATERIALS EXHIBITING STRUCTURAL COLOUR

BACKGROUND TO THE INVENTION

Field of the invention

The present invention relates to composite optical materials which demonstrate structural colour characteristics and to methods of manufacturing such composite optical materials.

Related art

Natural opal is built up from domains consisting of monodisperse silica spheres of diameter 150-400 nm. These spheres are close-packed and therefore form a regular three dimensional lattice structure within each domain. The colour play of such opals is created by Bragg-like scattering of the incident light at the lattice planes of the domains.

It is known to produce synthetic opal-like materials. For example, US-A-4,703,020 discloses the formation of such materials by allowing silica spheres to sediment from an aqueous dispersion. This sediment is then dried and calcined at 800°C. Subsequently, a solution of zirconium alkoxide is allowed to penetrate into the interstices in the sediment and zirconium oxide is precipitated in the interstices by hydrolysis. The material is then calcined again to leave a structure in which silica spheres are arranged in a three dimensional lattice with zirconium oxide in the interstices. Forming opal-like materials in this way is exceptionally time-consuming and expensive. It is not an industrially-applicable route for the manufacture of significant quantities of materials.

US 2004/0253443 (equivalent to WO03025035) discloses moulded bodies formed from core-shell particles. Each particle is formed of a solid core, and the solid cores have a monodisperse particle size distribution. Each particle has a shell formed surrounding the core. The core and shell have different refractive indices. In one embodiment in this document, the core is formed of crosslinked polystyrene and the shell is formed of a polyacrylate such as polymethyl methacrylate (PMMA). In this case, the core has a relatively high refractive index and the shell has a relatively low refractive index. A polymer interlayer may be provided between the core and shell, in order to adhere the shell to the core. Granules of the core-shell particles are heated and pressed to give a

film. In this heating and pressing step shell material is soft but the core material remains solid. The cores form a three dimensional periodic lattice arrangement, and the shell material becomes a matrix material. The resultant material demonstrates an optical opalescent effect. US 2004/0253443 suggests mechanisms to explain the ordering of the core particles in the matrix, but these are not fully explained.

US 2004/0253443, mentioned above, provides colloidal crystals by the self-assembly of monodispersed, submicrometer-sized beads. “Monodisperse” here means that the diameters of the beads are equal within a small deviation, preferably 3% of the mean diameter. Such beads usually crystallize in a face-centered cubic close packing which is commonly named an opal structure after the natural gemstone opal.

WO2004096894 provides similar disclosure to US 2004/0253443, and additionally proposes extruding the composite material as a sheet and subsequently rolling the material. The result is reported to be a uniform colour effect depending on the viewing angle.

Many security features of bank notes, passports, credit cards, brand labels and other documents are based on special colour features. Of special interest are dynamic colours which change with the orientation of the item to the viewer's eye. Although many materials are available to achieve a colour change with a variation of the viewing angle, materials which induce a change of colour by rotation of the item while the viewing angle remains constant are rare. US 2010/0045027 (equivalent to WO 2008/017869) discloses that this behaviour can be achieved by colloidal crystals that do not have a rotational symmetry about the normal to their surface.

The basic colours of opal-type colloidal crystals have been described earlier and are well understood. The “structural colour” characteristics arise because of scattering and interference of light at the lattice planes of the crystal. The colour depends on the set of lattice planes which scatter the light, and specifically the lattice constant of these lattice planes which in turn depends on the bead size and the angle under which the light meets the set of lattice planes. In an fcc structure, the strongest colour arises from the (111) lattice planes which are parallel to the surface of the specimen. This colour is dependent on the viewing angle, but invariant to a rotation of the sample. Colours which change with rotation of the specimen while keeping the viewing angle to the surface constant are

caused by lattice planes running in oblique angles through the three-dimensional crystal. However, the colour of these lattice planes is generally weak because of their low occupation with beads or the colour cannot be seen at all because total reflection at the surface prevents the reflected light from leaving the crystal.

Different approaches have been disclosed to produce polymer films with an internal opaline structure:

Asher et al (1994) [S. A. Asher, J. Holtz, L. Liu, Z. Wu "Self-Assembly Motif for Creating Submicron Periodic Materials. Polymerized Crystalline Colloidal Arrays" J. Am. Chem. Soc. 1994, 116, 4997-4998] disclosed the synthesis and possible applications of opal gels where monodispersed, charged polymer beads were crystallized in suspension and the dispersing liquid was subsequently crosslinked. Kumacheva et al (1999) [O. Kalinina, E. Kumacheva "A "Core-Shell" Approach to Producing 3D Polymer Nanocomposites" Macromol1999, 32, 4122-4129] disclosed opaline coatings made by the drying of aqueous suspensions of core-shell polymer beads and the subsequent heating of the coating until the shells flowed and formed a continuous matrix. A similar approach is described in US-B-6,337,131 (equivalent to EP-A-955323). Jethmalani and Ford (1996) [J. M. Jethmalani, W. T. Ford "Diffraction of Visible Light by Ordered Monodisperse Silica-Poly(methyl acrylate) Composite Films" Chem. Mater. 1996,8, 2138-2146] describe the preparation of colloidal crystals of silica beads embedded in poly methylmethacrylate films. Crystals of silica beads embedded in polymer films were also used to prepare polymer films with crystalline lattices of pores, the so-called inverse opals as described by Arsenault et al (2006) [A. C. Arsenault, T. J. Clark, G. von Freymann, L. Cademartiri, R. Sapienza, J. Bertolotti, E. Vekris, S. Wong, V. Kitaev, I. Manners, R. Z. Wang, S. John, D. Wiersma, G. A. Ozin "From colour fingerprinting to the control of photoluminescence in elastic photonic crystals" Nat Mater 2006, 5,179-184] and Jiang et al (2004) [P. Jiang, M. J. McFarland "Large-Scale Fabrication of Wafer-Size Colloidal Crystals, Macroporous Polymers and Nanocomposites by Spin-Coating" J. Am. Chem. Soc. 2004, 126, 50 13778-13786]. Jiang et al (2004) used a spin-coating technique for the preparation of the colloidal crystalline silica-polymer precursor films.

An advantage of the colloidal crystal films with continuous polymeric matrices is their deformability. Unlike in a suspension, deformation of a polymeric opal structure leads to a distortion of the whole lattice of the crystal. Depending on the kind and elasticity of the

polymer, the deformation can be large and reversible. Strain induced colour changes have been observed and described in the following literature:
Jethmalani and Ford (1996)
Ruhl and Hellman (2001) [T. Ruhl, G. P. Hellmann "Colloidal Crystals in Latex Films: Rubbery Opals" Macromol. Chem. Phys. 2001, 202, 3502-3505]
Viel at al (2007) [B. Viel, T. Ruhl, G. P. Hellmann "Reversible Deformation of Opal Elastomers" Chem. Mater. 2007, 19, 5673-5679;]
Pursiainen et al (2005) [O. L. J. Pursiainen, J. J. Baumberg, K. Ryan, J. Bauer, H. Winkler, B. Viel, T. Ruhl "Compact strain-sensitive flexible photonic crystals for sensors" Appl. Phys. Lett. 2005, 87, 101902]
Arsenault et al (2006)
Wohlleben et al (2007) [W. Wohlleben, F. W. Bartels, S. Altmann, R. J. Leyrer "Mechano-Optical Octave-Tunable Elastic Colloidal Crystals Made from Core-Shell Polymer Beads with Self Assembly Techniques" Langmuir 2007,23,2961-2969]
Ying and Foulger (2009) [Y. Ying, S. H. Foulger "Color characteristics of mechanochromic photonic bandgap composites" Sensors and Actuators B 2009, 574-577]

So far, academic and industrial interest has focused on the colour of the surface-parallel crystal planes (the (111) set of planes of the fcc lattice). With increasing strain, the wavelength of their reflection colour decreases and simultaneously its intensity decreases as well. At a high strain of about 60% or more, only a weak bluish-grey shade remains. The decrease of the wavelength under strain is considered to be due to the decrease in film thickness which leads to a decrease of the distance of the surface-parallel planes of the crystal lattice. The colour which is visible under limited strain remains invariant to a rotation of the specimen: Although the strain distorts the fcc lattice and lowers its symmetry, the surface parallel lattice planes retain their rotational symmetry about the normal to the surface. An explanation of the loss of colour at high strain was given by Viel et al (2007), namely that large strain could randomize the ABC-like stacking of the close-packed layers of the fcc crystal, thereby destroying the three-dimensional order.

SUMMARY OF THE INVENTION

The present inventors consider that it is of interest to further develop composite optical materials in order to provide a composite optical material that displays structural colour that varies with rotation of the material about an axis perpendicular to the surface of the material, even when the viewing angle remains constant. Such materials would be of interest for various applications, including security applications such as on financial instruments and documents.

The present invention has been devised in order to address the want of such a composite optical material. Further advantages, and/or problems that may be solved by the present invention, are set out in more detail below.

Accordingly, in a first preferred aspect, the present invention provides a composite optical material having a three dimensional arrangement of core particles distributed in a matrix, the refractive index of the material of the core particles being different to the refractive index of the material of the matrix and the three dimensional arrangement having a periodicity such that, when a surface of the material is illuminated with white light, the composite material exhibits structural colour, wherein the three dimensional periodic arrangement is a reduced symmetry arrangement based on a crystallographic close-packed arrangement but strained therefrom to have reduced symmetry about a rotational axis perpendicular to the surface compared with the crystallographic close-packed arrangement so that Bragg reflections from planes disposed at oblique angles to the surface that would be forbidden in the crystallographic close-packed arrangement or would be subject to total internal reflection at the surface are allowed and visible from the reduced symmetry arrangement, thereby providing a variation in intensity and/or wavelength of structural colour with rotation of the material about an axis perpendicular to the surface when viewed obliquely while the viewing angle remains substantially constant.

In a second preferred aspect, the present invention provides a method for manufacturing a composite optical material, the method including the steps:

in a first configuration of the composite optical material, providing a crystallographic close-packed arrangement of core particles distributed in a matrix, the refractive index of the material of the core particles being different to the

refractive index of the material of the matrix and the arrangement having a periodicity such that, when a surface of the material is illuminated, the arrangement exhibits Bragg reflection, optionally in the visible spectrum, the crystallographic close-packed arrangement having a degree of symmetry such that Bragg reflections from at least one set of crystallographic planes are forbidden or are subject to total internal reflection at the surface;

transforming the first configuration of the composite optical material to a second configuration by straining the crystallographic close-packed arrangement to provide a reduced symmetry arrangement having reduced symmetry about a rotational axis perpendicular to the surface compared with the crystallographic close-packed arrangement so that Bragg reflections from planes disposed at oblique angles to the surface that were forbidden in the crystallographic close-packed arrangement or subject to total reflection at the surface are allowed and visible from the reduced symmetry arrangement.

In a third preferred aspect, the present invention provides a composite optical material obtained by, or obtainable by, a method according to the second aspect.

In a fourth preferred aspect, the present invention provides a composite optical material, having a first configuration and a second configuration, wherein:

in the first configuration, a crystallographic close-packed arrangement of core particles is provided distributed in a matrix, the refractive index of the material of the core particles being different to the refractive index of the material of the matrix and the arrangement having a periodicity such that, when a surface of the material is illuminated, the arrangement exhibits Bragg reflection, optionally in the visible spectrum, the crystallographic close-packed arrangement having a degree of symmetry such that Bragg reflections from at least one set of crystallographic planes are forbidden or are subject to total internal reflection at the surface; and

in the second configuration, the crystallographic close-packed arrangement is strained to provide a reduced symmetry arrangement having reduced symmetry about a rotational axis perpendicular to the surface compared with the crystallographic close-packed arrangement so that Bragg reflections from planes disposed at oblique angles to the surface that were forbidden in the

crystallographic close-packed arrangement or subject to total reflection at the surface are allowed and visible from the reduced symmetry arrangement,

the composite optical material being reversibly deformable from the first configuration to the second configuration.

Preferred and/or optional features of the invention will now be set out. These are applicable singly or in any combination with any aspect of the invention, unless the context demands otherwise.

With respect to the first aspect, when sufficiently deformed, the material preferably mechanically fails before the strain of the deformation is sufficient to force the reduced symmetry arrangement to return to rotational symmetry of the crystallographic close-packed arrangement.

For example, the material may fail by tearing, cracking or localised plastic yielding. Thus, at least with respect to the first aspect, it is preferred that the reduced symmetry arrangement is substantially irreversible in the composite optical material. This is advantageous for security device applications, e.g. to reduce the risk of tampering with the security device.

With respect to the second aspect, the method further includes the step of treating the composite optical material in order to constrain the reduced symmetry arrangement from returning to the crystallographic close-packed arrangement.

Such treatment may include increasing the stiffness of the matrix material in the second configuration compared with the stiffness of the matrix material in the first configuration.

For example, the matrix material may be treated by cross-linking treatment. This is a convenient approach to allowing suitable deformation of the material to adopt the second configuration and then to allow fixing of the second configuration. Suitable cross-linking treatment can be carried out by incorporation of a suitable cross-linking component in the matrix material, e.g. a UV-activatable cross-linking component.

Additionally or alternatively, the matrix material may be treated to raise the glass transition temperature (Tg) of the matrix material. This may be done by removing a

softening component from the matrix (e.g. by evaporation on heating). This has a similar effect to cross-linking, explained above.

Additionally or alternatively, the matrix may be in the first configuration above Tg of the matrix material, and then cooled to below Tg in the second configuration. This has a similar effect to cross-linking, explained above.

Additionally or alternatively, the composite optical material may be permanently bonded to a support, in order to hold the matrix material and thus prevent return of the reduced symmetry arrangement to the crystallographic close-packed arrangement. This is an attractive option where the composite optical material is in the form of a film or layer and is intended to be affixed to a support, e.g. to provide an indication of the authenticity of the support, such as a banknote.

The core particles are disposed in the composite optical material in an arrangement based on a three dimensional crystallographic close packed lattice. Preferably the core particles are disposed in the composite material in an arrangement based on a face centred cubic lattice. Preferably, a {111} plane (nominally the (111) plane) of the lattice is aligned substantially parallel to a major surface of the composite optical material. By "major surface" it is intended that the composite optical material is in the form of a sheet, film or layer.

Preferably, the step of transforming the first configuration of the composite optical material to the second configuration includes the step of straining the crystallographic close-packed arrangement along a direction that is not parallel to a close packed direction in the crystallographic close-packed arrangement. By "close packed direction in the crystallographic close-packed arrangement", it is intended to refer to the lines of close packing that occur in crystallographic close-packed arrangements. In crystal structures where the (111) plane is a close packed plane, for example, the close packed directions contained in the (111) plane are <110> type directions.

More preferably, the step of transforming the first configuration of the composite optical material to the second configuration includes the step of straining the crystallographic close-packed arrangement along a direction that is substantially perpendicular to a close packed direction in the crystallographic close-packed arrangement. In crystal structures

where the (111) plane is a close packed plane, for example, the directions perpendicular to close packed directions are <221> type directions. Specifically, where the close packed direction of interest is [10-1], which lies in the (111) plane, for example, the perpendicular directions are [1-21 and [-12-1].

Preferably, the strain applied to the composite optical material is tensile strain.

It is considered that similar effects may be observed when shear strain is applied along a corresponding direction. Furthermore, it is considered that similar effects may be observed when compressive strain is applied along a corresponding direction.

Preferably, the strain applied during the step of transformation from the first configuration to the second configuration is at least 40%. More preferably, the strain applied during the step of transformation from the first configuration to the second configuration is at least 50%, still more preferably at least 60%. As will be appreciated, this amount of strain is extremely high. The present inventors have found that even under such high strain, the strain is taken up substantially homogeneously by the composite optical material, allowing similar crystalline transformations and/or crystalline reorientation to occur across the composite optical material and thereby ensuring that the structural colour exhibited is substantially uniform across the composite optical material.

The composite optical material is typically formed (as explained elsewhere in this disclosure) by shear processing of a precursor composite material. It has been found that suitable ordering of the core particles in the matrix can be obtained by repeated shearing back and forth along a shear processing direction. Such processing tends to produce a composite optical material in which a close packed direction is parallel to the shear processing direction. Thus, it is further preferred that the strain applied during the step of transformation from the first configuration to the second configuration is not parallel to the shear processing direction. More preferably, the strain applied during the step of transformation from the first configuration to the second configuration is substantially perpendicular to the shear processing direction.

The primary reflections from the material in the unstrained configuration are typically (111) reflections for an fcc lattice. However, it is found that the reflection from these planes, which are typically parallel to the surface, are strongest when the viewing angle

and the illumination angle are the same. However, the gloss and the remission of the surface are strongest in the same direction. Therefore, the (111) colour is usually impaired by background light, typically white background light. This reduces the perceived intensity of the (111) structural colour. However, when reflections are seen from oblique planes, in accordance with the preferred embodiments, the structural colour appears on a darker background, because the gloss and remission of the surface typically are not strong in the directions in which the structural colour from those oblique planes are strongest.

Bragg reflection in polymer opals tends to be strongest for the most densely populated crystal planes. Therefore reflection is strongest from the {111} close packed planes. The reason why planes such as (-111) do not show structural colour in polymer opal films is due to their orientation with respect to the surface of the film. Any light reflected from these planes meets the surface at an angle which provides total internal reflection. Therefore this light is consumed within the film and is not allowed to escape from the surface. However, if the strain of the material is sufficient to re-orient the (-111) plane to an angle relative to the surface so that total internal reflection no longer occurs at the surface for light reflected from these planes, then the (-111) plane exhibits structural colour.

It is possible to relate the intensity of the reflections from the reduced symmetry arrangement (i.e. the second configuration) to that of the close packed arrangement (i.e. the first configuration). Normalised to the unstrained (111) reflection intensity, the intensity of at the reflections from the reduced symmetry arrangement in at least one oblique viewing direction is at least 0.1, more preferably at least 0.2. At the same strain, normalised to the unstrained (111) reflection intensity, it is typical for the (111) reflections from the reduced symmetry arrangement to have a maximum intensity of about 0.6. In preferred embodiments, the intensity of at the reflections from the reduced symmetry arrangement in at least one oblique viewing direction is substantially the same as the (111) reflections from the same reduced symmetry arrangement.

Preferably, the reflections from the oblique planes visible in the reduced symmetry arrangement are seen in a range of rotational angles of about ±25° from a maximum intensity of the reflections.

Preferably, the reflections from the oblique planes visible in the reduced symmetry arrangement are seen in a range of tilt angles of about ±13° from a maximum intensity of the reflections.

Rotational and tilt angles are explained in Fig. 3.

It is well known in the field of crystallography (particularly from X-ray and electron diffraction studies) that crystal structures with high degrees of symmetry have certain "selection rules" that can be used to determine whether reflections from certain classes of crystallographic planes will be exhibited.

For an fcc lattice, based on the Miller indices h, k and l for a family of crystallographic planes {hkl}, Bragg reflections are allowed where h, k and l are all odd or all even, but Bragg reflections are forbidden when h, k and l are mixed odd and even. (Here, 0 counts as an even number.) For example, in an fcc lattice, {111}, {200} and {311} Bragg reflections are allowed, but {110}, {211} and {221} reflections are forbidden.

Thus, where the first configuration of the composite optical material has an fcc structure, preferably the second configuration exhibits Bragg reflection from at least one set of planes that would be forbidden in an fcc structure.

In some embodiments, although without wishing to be bound by theory, the inventors speculate that the crystallographic structure of the composite optical material in the second configuration is a monoclinic structure.

Preferably, the core particles have a difference in refractive index compared with the matrix material, of at least 0.001, more preferably at least 0.01, still more preferably at least 0.1.

In some embodiments, in order to form the composite optical material, there is provided a population of core-shell particles. Each core-shell particle preferably comprises a core and a shell material surrounding the core. The population may take the form of granules. Preferably, the population is heated to a temperature at which the shell material is flexible and soft. The population is then preferably subjected to the action of a mechanical force to initiate three dimensionally periodic arrangement of the core particles

in a matrix of the shell material. This mechanical force is preferably provided by an extrusion process. The result of the extrusion process is typically a ribbon of precursor composite material.

Preferably, the ribbon of precursor composite material is captured and held between first and second sandwiching layers. The resulting structure may then be rolled (or calendered or otherwise pressed) in order to cause the precursor composite material to flow further. In some embodiments (e.g. for films of thickness greater than about 200 μm), suitable structural colour can be achieved at this point in the process and further colour enhancement steps may not be necessary.

If a further colour enhancement step is needed or desired, the composite material is then preferably allowed to cool to a temperature at which the shell material is no longer soft. The resulting sandwich structure can then be subjected to further processing in order to provide the required degree of periodicity of the core particles in the matrix. Such a subsequent colour enhancement step is considered to be suitable for thin opal films (e.g. of thickness less than 200 μm) which are preferred in some embodiments of this invention.

Other processes can be used in place of extrusion. For example, the action of mechanical force may take place via one or more of: uniaxial pressing (e.g. forming a film or plate); injection-moulding; transfer moulding; co-extrusion; calendering; lamination; blowing; fibre-drawing; embossing; and nano-imprinting.

When the action of force takes place through uniaxial pressing, the precursor composite material is preferably in the form of a film or layer. Suitable films or layers can preferably also be produced by calendering, film blowing or flat-film extrusion.

When the precursor composite material is produced by injection moulding, it is particularly preferred for the demoulding not to take place until after the mould with moulding inside has cooled. When carried out in industry, it is advantageous to employ moulds having a large cooling-channel cross section since the cooling can then take place in a relatively short time. The mould may advantageously be heated before the injection operation.

The processes set out above rely on mechanical shearing of the film in order to produce the required periodicity in the film. However, other processes are also possible. For example, a dispersion (e.g. an aqueous dispersion) of the core-shell particles can be dried in order to form the required film. Because of the absence of shear, the orientation of the lattice is not so easy to obtain as in the processes discussed above. Typically, the (111) planes form the surface of the film, but for further orientation (closely packed strips of particles a discussed below for the shear processes) a directional, vertical drying is carried out as described in Jiang et al (1999) [Jiang, P.; Bertone, J. F.; Hwang, K. S.; Colvin, V. L. "Single-Crystal Colloidal Multilayers of Controlled Thickness" Chem. Mater. 1999, 11, 2132-2140] and Wohlleben (2007) [Wendel Wohlleben, Frank W. Bartels, Stephan Altmann, and Reinhold J. Leyrer "Mechano-Optical Octave-Tunable Elastic Colloidal Crystals Made from Core-Shell Polymer Beads with Self-Assembly Techniques" Langmuir 2007, 23, 2961-2969]. In this process, the film can be formed of polystyrene-polyethylacrylate core shell particles.

Preferably, the core particles have a substantially monodisperse size distribution. The size of the core particles depends on the intended wavelength(s) at which the composite optical material should provide the required optical effect(s). For example, it may be desirable for the core particles to have a mean particle diameter in the range from about 5 nm to about 2000 nm. More preferably, the core particles have a mean particle diameter in the region of about 50-500 nm, more preferably 100-500 nm. Still more preferably, the core particles have a mean particle diameter of at least 150 nm. The core particles may have a mean particle diameter of at most 400 nm, or at most 300 nm, or at most 250 nm.

Preferably, the material of the core particles remains substantially rigid and substantially undeformed during the process. This can be achieved by: using a high crosslinking density in the core particles; and/or by using processing temperatures below the glass transition temperature (Tg) of the core material.

Thus, it is possible to use materials with a relatively low Tg for the core particles, provided that their degree of crosslinking is sufficient to avoid deformation of the core particles at the processing temperature using the method of the invention. A suitable degree of crosslinking may be, for example, 1% crosslinking density or higher. More

preferably, the degree of crosslinking is 2% or more, more preferably about 10% crosslinking density.

Alternatively, although this is not necessarily preferred, inorganic core materials may be used.

Preferably, the shell of the core-shell particles is bonded to the core via an interlayer.

Suitable composite optical materials may be manufactured by suitable shearing of the precursor composite material, typically between first and second sandwiching layers. For example, one suitable approach is to deform the precursor composite material progressively and repeatedly over a hot edge. This is disclosed, for example, in WO 2011/004190, the contents of which are incorporated herein by reference in their entirety. Another suitable approach is to deform the precursor composite material by repeated curling, as disclosed in GB patent application 1100506.3, filed 12 January 2011 and unpublished at the time of writing this disclosure, the contents of which are incorporated herein by reference in their entirety.

It is considered that the ordering of the core particles in the precursor composite material begins preferentially at the interfaces between the precursor composite material and the sandwiching layers. During the process, it is considered that the ordering then extends inwards into the precursor composite material. Therefore, at large thickness values, precise ordering of the material at the centre of the structure may not be achievable. However, for such large thickness values, this may not be a problem because there will be very many ordered layers nearer the interfaces with the sandwiching layers. Preferably, the thickness of the composite optical material is at most 1 mm. More preferably, the thickness of the composite optical material is at most 0.5 mm, or at most 0.4 mm, or at most 0.3 mm. The thickness of the composite optical material is preferably at least 10 μm, since thinner structures may not have sufficient mechanical integrity for practical uses and may not provide sufficiently strong reflections in order to exhibit a significant structural colour effect. More preferably, the thickness of the composite optical material is at least 20 μm, or at least 30 μm, or at least 40 μm, or at least 50 μm, or at least 60 μm, or at least 70 μm, or at least 80 μm. A thickness of about 100 μm has been found to be suitable, for example.

The composite optical material and/or the precursor composite material may comprise auxiliaries and/or additives. These can serve in order to provide desired properties of the body. Examples of auxiliaries and/or additives of this type are antioxidants, UV stabilisers, biocides, plasticisers, film-formation auxiliaries, flow-control agents, fillers, melting assistants, adhesives, release agents, application auxiliaries, demoulding auxiliaries and viscosity modifiers, for example thickeners, pigments and fillers.

Preferably, one or more species of nanoparticles is included in the matrix material, in addition to the cores of the core-shell particles. These particles are selected with respect to their particle size in such a way that they fit into the cavities of the packing (e.g. sphere packing) of the core particles and thus cause only little change in the arrangement of the core particles. Through specific selection of corresponding materials and/or the particle size, it is firstly possible to modify the optical effects of the composite optical material, for example to increase its intensity. Secondly, it is possible through incorporation of suitable "quantum dots", to functionalise the matrix. Preferred materials are inorganic nanoparticles, in particular carbon nanoparticles (e.g. carbon nanotubes), nanoparticles of metals or of II-VI or III-V semiconductors or of materials which influence the magnetic/electrical (electronic) properties of the materials. Examples of further preferred nanoparticles are noble metals, such as silver, gold and platinum, semiconductors or insulators, such as zinc chalcogenides and cadmium chalcogenides, oxides, such as haematite, magnetite or perovskite, or metal nitrides, for example gallium nitride, or mixed phases of these materials. Furthermore, the matrix material can include one or more dyes. A suitable dye may be fluorescent.

Preferably, the nanoparticles have an average particle size of 50 nm or less. The nanoparticles may have an average particle size of at least 5 nm. An average particle size in the range 10-50 nm (e.g. about 20 nm) has been found to give suitable results. Preferably, the proportion by weight of the nanoparticles in the composite is less than 1%, more preferably less than 0.5%, less than 0.1% and still more preferably less than 0.01%. The nanoparticles preferably are distributed uniformly in the matrix material.

Preferably, the interlayer is a layer of crosslinked or at least partially crosslinked polymers. The crosslinking of the interlayer here can take place via free radicals, for example induced by UV irradiation, or preferably via di- or oligofunctional monomers.

The crosslinked or partially crosslinked interlayer provides reactive functions for the grafting of polymer chains of the shell polymer. It is preferred to use the same functional groups for crosslinking of the interlayer and for the grafting of the shell polymer. Preferred interlayers in this embodiment comprise from 0.01 to 100% by weight, particularly preferably from 0.25 to 10% by weight, of di- or oligofunctional monomers. Grafting can also be obtained by using di- or oligofunctional monomers in the core, but this is not preferred as more of the di- or oligofunctional monomer is needed. Suitable di- or oligofunctional monomers are, in particular, isoprene and allyl methacrylate (ALMA). The interlayer preferably has a thickness in the range from 10 to 20 nm. Thicker interlayer materials may be possible.

Preferably the shell is formed of a thermoplastic or elastomeric polymer. Since the shell essentially determines the material properties and processing conditions of the core-shell particles, the person skilled in the art will select the shell material in accordance with the usual considerations in polymer technology, but with particular attention to the requirement that there should be a significant refractive index difference compared with the core material, in order to provide spectral colour.

The core particles are preferably spherical, or substantially spherical, in shape. Preferably, the distribution of the diameter of the core particles is substantially monodisperse, e.g. with a standard deviation of 20% or less, more preferably 10% or less, more preferably 5% or less, still more preferably 3% or less.

It can be advantageous for the core : shell volume ratio to be in the range from 2:1 to 1:5, preferably in the range from 3:2 to 1:3 and particularly preferably in the region below 1.2:1. In specific embodiments of the present invention, it is even preferred for the core:shell volume ratio to be less than 1:1, to assist the melt processing in therms of allowing the cores to move in the matrix. Where an interlayer is provided, preferably the volume of core and interlayer present in the material is less than 50 vol%, e.g. about 45 vol%.

Further optional features of the invention are set out below.

BRIEF DESCRIPTION OF THE DRAWINGS

Preferred embodiments of the invention will be set out by way of example with reference to the drawings, in which:

Figs. 1 and 2 illustrate an optical effect exhibited by a composite optical material film according to a preferred embodiment of the invention.

Fig. 3 illustrates the viewing arrangement for composite optical material films treated according to preferred embodiments of the invention.

Figs. 4-7 illustrate a simple representation of the optical effect of three composite optical material films according to an embodiment of the invention.

Figs. 8A-10A show the evaluation of a series of UV/visible spectra taken at different rotation angles for a composite optical material film according to an embodiment of the invention.

Figs. 8B-10B show the evaluation of a series of UV/visible spectra taken at different tilt angles for a composite optical material film according to an embodiment of the invention.

Figs. 11A and 11B illustrate two principal axes of the composite optical material considered in the preferred embodiments.

Fig. 12 shows stress-strain curves for strip of composite optical materials according to embodiments of the invention stretched along the p^ and n^ directions, at rates of 10 and 200 μms^{-1}. Fig. 13 shown Poisson's ratio for the same strips as in Fig, 12, in-plane (y) and perpendicular to the plane (z).

Figs. 14A and B shows dark-field Bragg scattering spectra as uniaxial strain increases for composite optical materials according to embodiments of the invention, using contours ε along the (a) p^ and (b) n^ directions. The inset in Fig. 14B shows selected dark-field spectra as strain increases. Fig. 14C shows peak scattering wavelength and Fig. 14D shows extracted linewidths, for strain in each direction. The dotted line in Fig. 14D shows yield strain. The inset in Fig. 14C shows reduction in scattering efficiency with

strain. The inset in Fig. 14D shows movement of (111) plane spheres for different strain directions.

Fig. 15 shows a schematic hard-sphere model, showing how extension along [-101] (arrows along face of sample film) leads to shear along (-11-1) (arrows along plane inclined to face of sample film and solid arrows in inset), which pulls close-packed planes apart enough to allow slip (open arrow in inset).

DETAILED DESCRIPTION OF THE PREFERRED EMBODIMENTS, FURTHER OPTIONAL FEATURES OF THE INVENTION

The entire content of each the documents referred to in any section of this disclosure is hereby incorporated by reference.

The present inventors have surprisingly found that appropriate elastic polymer films consisting of a colloidal-crystalline fcc lattice of core particles (sometimes referred to as beads), stretched in a certain direction, show at high strain strong colour which it is not only dependent on the viewing angle, but also on a rotation of the sample. To the knowledge of the inventors, both strong colour under strain and strong dependency on rotation have so far not been disclosed for any opal-type colloidal crystals.

The rubber-like opal films disclosed in US-B-6,337,131 (equivalent to EP-A-955323) and US 2004/0253443 (equivalent to WO03025035 and EP-B-1425322) were found to be particularly applicable. They consist of monodisperse polymer core particles embedded and crystallized inside a matrix of soft polymer which renders the so-called "opal films" or "rubbery opals" easily deformable. Their deformation under strain is uniform and can propagate through the whole film (particularly so when the whole film consists of a single domain). The melt-processing technique disclosed in US 2004/0253443 is especially suited to yield large area samples with well-known orientation of the colloidal crystal lattice.

In the simplest case this melt-processing is carried out by pressing a molten mass of core-interlayer-shell particles between two flat metal sheets covered with a protective foil to prevent sticking. The melt flows outwards and the particles crystallize forming a colloidal crystalline opal film disc while the polymer shells coalesce to form a continuous

polymer matrix. The synthesis of the core-interlayer-shell beads and the preparation of the opal disks has been described in detail in Ruhl and Hellmann (2001) and Ruhl et al (2003) [T. Ruhl, P. Spahn, G. P. Hellmann "Artificial opals prepared by melt compression" Polymer 2003, 44, 7625-7634].

To achieve a high strain of greater than 10% (and preferably much greater than 10%) without cracking, the shell polymer of the beads which forms the matrix of the opal films should have a Glass Transition Temperature Tg which is lower than the temperature of the film during the deformation. For a given Tg, e.g. Tg > 60°C for opal films which are solid at room temperature, the temperature during the deformation should be adjusted appropriately. If the temperature during the deformation is fixed, e.g. ambient temperature (typically taken to be 23°C), a suitable composition of the shell polymer can be chosen to adjust Tg. The adjustment of Tg by a variation of the polymer composition is well known to the specialist and industrial standard. For emulsion polymerization, it is described e.g. in "Waßrige Polymerdispersionen : Synthese, Eigenschaften, Anwendungen" Dieter Distler, Weinheim ; New York; Chichester; Brisbane; Singapore; Toronto: Wiley-VCH, 1999. Emulsion polymerization is a suitable technique for the formation of the core-shell particles.

Many acrylic, methacrylic, styrenic, vinyl and other monomers are available for the emulsion polymerization. The present inventors have found that comonomers of ethyl acrylate and iso-butyl methacrylate are especially appropriate as shell polymers. Both react quickly and completely during the emulsion polymerization. The ethylacrylate lowers the Tg and yields soft, elastic polymers. Poly ethylacrylate has a refractive index of n = 1.47. The iso-butyl methacrylate increases the Tg while the refractive index of the copolymer remains low. Poly-iso-butylmethacrylate has a refractrive index of 1.45. Copolymers of ethylacrylate and iso-butylmethacrylate can be varied between soft and sticky, very elastic through tough and leatherlike to brittle.

The crystal lattice orientation inside the opal discs was determined by Pursiainen et al (2008) [O. L. J. Pursiainen, J. J. Baumberg, H. Winkler, B. Viel, P. Spahn, T. Ruhl "Shear-Induced Organization in Flexible Polymer Opals" Adv. Mater. 2008, 20, 1484-1487] and by Ruhl et al (2004) [T. Ruhl, P. Spahn, H. Winkler, G. P. Hellmann "Large Area Monodomain Order in Colloidal Crystals" Macromol. Chem. Phys. 2004, 205, 1385-1393]. The main characteristics of the crystal lattice orientation are:

(a) The surface of the opal disc contains close packed beads

(b) Each radial sector can be seen as a single crystal of the fcc lattice

(c) The (111) planes of the fcc lattice run parallel to the surface

(d) Close packed lines of beads run radially along the surface

As mentioned above, an alternative route for the preparation of thin opal tapes by extrusion, calendering and an additional colour enhancement step has been disclosed in WO 2011/004190, the contents of which are incorporated herein by reference in their entirety. Another suitable approach is to deform the precursor composite material by repeated curling, as disclosed in GB patent application 1100506.3, filed 12 January 2011 and unpublished at the time of writing this disclosure, the contents of which are incorporated herein by reference in their entirety. The shearing process in these disclosures does not provide radial flow of the precursor composite material. As such, the orientation of the fcc lattice is different compared with the simpler approach of pressing a molten mass of the material. In these disclosures, the (111) planes are still parallel to the film surface but the close packed lines of beads run along the length of the film (i.e. parallel to the shear processing direction).

The present inventors have found that where a subsequent strain of sufficient magnitude is applied either parallel or perpendicular to the close packed directions, different effects are seen. Specifically, an effect is seen when the strain is applied perpendicular to the close packed direction that is not seen when the strain is applied parallel to the close packed direction. The inventors found that a novel kind of structural colour, dependent on viewing angle and on rotation of the sample appears when strain is applied normal to the dense packed lines of beads.

The effect is illustrated in Figs. 1 and 2. A sample film, cut from an opal disk, is strained normal to the lines of close packed beads. Fig. 1 illustrates images taken in plan view (normal to the surface of the film) showing schematically (using black and white shading) the shift of the reflection colour to shorter wavelengths with increasing strain. The same sample film is illustrated in each view, with the strain progressively increasing from left to right across Fig. 1. The colour changes from a strong red (Fig. 1 original) to orange (Fig. 1 ε=10%) to green (Fig. 1 ε=20%) to turquoise (Fig. 1 ε=35%) to deeper turquoise (Fig. 1 ε=50%) to blue (Fig. 1 ε=63%).

At the high strain of ε=63%, a view of the strained sample film from the side reveals a new, strong red colour. This view is illustrated schematically in Fig. 2. This colour is especially striking as it appears as a kind of backscattering on a relatively dark background. It is not impaired by the surface gloss of the polymer film.

Fig. 3 illustrates the viewing arrangement for composite optical material films treated according to preferred embodiments of the invention. Composite optical material (polymer opal) film 10 has a substantially planar upper major surface. The film 10 is illuminated with white light. A small area of the film is observed via optical fibre 12. Optical fibre 12 is oriented so as to define a plane with the axis N normal to the planar upper surface of film 10. The angle in this plane between the axis N and the optical fibre is the viewing angle V. In Fig. 3, viewing angle V (represented by a square symbol) is 50°. The optical fibre can be rotated about the axis N. This defines the angle of rotation R of the optical fibre. As shown in Fig. 3, R is variable between 0 and 180°. Thus, using the arrangement in Fig. 3, it is possible to observe the sample film at a predetermined (and fixed) viewing angle, and to rotate the direction of observation whilst maintaining the viewing angle constant.

A simple representation of the effect of an embodiment of the invention is shown in Figs. 4-7, in which three polymer opal samples A, B and C are strained along their length, perpendicular to a close packed direction, and affixed to a support (in this case the samples are fixed to a paper substrate using sticky tape). As between Figs. 4-7, the samples are not changed. The only thing that is changed is the direction of viewing of the samples. The viewing angle is maintained substantially constant and the rotation angle is progressed from about 0° to about 90°.

In Fig. 4, each one of the samples A, B and C does not exhibit structural colour in the viewing direction of Fig. 4.

Fig. 5 is rotated compared with Fig. 4. Although samples A and C do not exhibit structural colour in the viewing direction of Fig. 5, sample B shows a red structural colour.

Fig. 6 is rotated compared with Fig. 5. Although samples A and B do not exhibit structural colour in the viewing direction of Fig. 6, sample C shows a strong red structural colour.

Fig. 7 is rotated compared with Fig. 6. Although sample B does not exhibit structural colour in the viewing direction of Fig. 7, sample A shows a strong red structural colour and sample C shows a weaker red structural colour than in Fig. 6.

The properties of this new structural colour effect have been investigated further by the inventors. Figs. 8A-10A show the evaluation of a series of UV/visible spectra taken at different rotation angles. Fig. 8A shows a contour map of the intensity of the structural colour effect and the peak wavelength of the structural colour effect with rotation. Fig. 10A shows a line plot of the intensity of the structural colour effect with rotation. Fig. 9A shows a line plot of the peak wavelength of the structural colour effect with rotation.

Fig. 8B shows a contour map of the intensity of the structural colour effect with tilt of the sample. This measurement shows at about 0° the reflection of (111) plus the surface gloss effect (mirror image of light source) and at about 50° tilt the backscattering reflection from oblique planes. The intensities of these reflections are similar, and confirmed by Fig. 10B. Fig. 9B shows a line plot of the peak wavelength of the structural colour effect with tilt.

For many applications a fixation of the second configuration (the strained state) is advantageous, in order that the user does not need to strain the composite optical material in order to reveal the new structural colour effect. Some suitable methods for achieving suitable fixation of the second configuration are:

- Sticking/gluing/bonding the strained film onto a solid support
- Cooling the strained sample below the Tg of the matrix polymer
- Increasing the Tg of the matrix polymer by the evaporation of a softener
- Crosslinking of the matrix polymer

The new type of viewing angle-dependent and rotation-angle dependent structural colour has many applications. The structural colour effect is strong especially as it appears as a kind of backscattering. These composite optical material films are suitable as security features for banknotes, passports, credit cards, brand labels and other applications or as lettering on signs which are readable only from a certain direction.

The present inventors have further investigated the likely mechanism behind the novel effect exhibited by the preferred embodiments.

As explained in more detail below, both the mechanical and optical properties of the material in the second configuration are found to be anisotropic, depending on the specific stretch direction relative to the close-packed particles in the close-packed (111) planes.

The present inventors find that a sphere-packing model predicts the low-strain behaviour < 40% strain. This model is unable to account for the phase transitions observed > 40% strains but predicts the findings for low strain accurately.

Shear-assembled fcc lattices of 200-nm polymer spheres within single-domain elastomeric films were distorted. The inventors consider, without wishing to be bound by theory, that suitable distortion induces phase transitions to an anisotropic monoclinic state at strains ≤ 40%. The transition to a lower-symmetry state breaks the traditional diffraction rules of fcc lattices, "turning on" unusual structural colour scattering in specific orientations.

Polymer opal crystalline films are produced by shear assembly of hard-core or soft-shell nanoparticles resulting in the growth of highly ordered (111) planes from a film surface. Compression, extrusion, and rolling can yield films of high order, and these techniques have been optimized to produce the current films. The mechanism of such highly ordered shear-induced assembly is still under study, but the consistent anisotropies observed here match theory for a perfect fcc film and support the full 3D order suggested by spectroscopy and microscopy. Such films, which have now been produced on the 100-m length scale, result in intense structural colour coming from the Bragg scattering peak.

Here, two principal axes are considered, as illustrated in Figs. 11A and 11B. Fig. 11A illustrates a direction ($\hat{p} = [\bar{1}01]$) parallel to the shear processing direction. Fig. 11B illustrates a direction ($\hat{n} = [1\bar{2}1]$) normal to the shear processing direction. The shear processing direction referred to here is the shear processing that is used to control the fcc self-assembly. Elsewhere in this disclosure, the Miller indices incorporating negative

numbers such as $[1\bar{2}1]$ are written as [1-21], simply for formatting reasons. Similarly, elsewhere in this disclosure $\hat{p}$ is written p^ and $\hat{n}$ is written n^.

Strips of 2.5-cm-wide films were cut in different orientations to the close-packed line of spheres in the (111) hexagonally packed plane. Using a 257-nm UV laser to record surface diffraction patterns (since the UV propagates <500 nm through the polymers before absorption), sixfold-symmetric patterns were always obtained, confirming the above orientations relative to the ordered lattice. Uniaxial strain ε was applied to each of these strips on a tensile stress stage under a microscope, allowing images and spectra to be recorded synchronously as the force is applied. An image-tracking algorithm was used to extract the actual locally induced strains both parallel and normal to the applied strain. The algorithm locates the positions of impurities and imperfections observed in real-time microscope images of the polymer film and tracks their relative coordinates as they move. Hence, together with the spectroscopy which measures the planar spacing vertically, the full strain distortions could be directly tracked in real time.

Fig. 12 shows stress-strain curves for strips stretched along the p^ and n^ directions, at rates of 10 and 200 μms^{-1}. Fig. 13 shown Poisson's ratio for the same strips as in Fig, 13a, in-plane (y) and perpendicular to the plane (z).

The mechanical response of the polymer films produces anisotropic stress-strain curves for the two different strain directions (see Fig. 12), taken at the two different strain rates. It is emphasized that such reproducible anisotropic behaviour depends on high crystalline order throughout the samples. Although the yield stress trebles with this increase in strain rate, the yield strain and shape are unaffected, suggesting their intrinsic origin. While the non-cross-linked soft-shell material deforms under stress, the strongly cross-linked core material is hard and non-deformable. Shells of adjacent particles are not chemically bonded together, and so particle rearrangement is possible by applying shear stress. As discussed above, fixing of the lower symmetry arrangement of the particles is preferred in some embodiments, e.g. by cross-linking of the matrix material after transformation of the material to the second configuration. Note that for the brittle sphere core material, the stress-strain curve would be a vertical line on the scale shown in Fig. 12, while the soft sticky shell material on its own follows a near-horizontal line. The ordered particle composite thus acquires distinctly new anisotropic properties compared to its component materials.

The extracted Young's modulus was found to be isotropic in the fcc crystal for these symmetry directions as expected. However, it becomes anisotropic under strain when the crystal may be considered to become monoclinic, as discussed below. Despite this anisotropy, the crystal yields at similar strains ε = 20% for both strain directions, implicating an intrinsic mechanism. For larger strains the material exhibits a soft elasticity with significant anisotropy and shows more strain hardening for ε >70% along the n^ direction. The extracted Poisson ratio (see Fig. 13) is also anisotropic, with larger contraction along the y direction when stretched along p^ and faster z compression of the layers when stretched along n^. These characteristics are addressed in the model developed below.

Because of the tight coupling between mechanical and optical properties of these photonic crystals, their anisotropic behaviour extends to the observed optical domain. Strain changes the lattice plane spacing in different directions, and may lead to reorientation of the lattice planes, leading to new scattering effects visible from the film.

Figs. 14A and 14B shows dark-field Bragg scattering spectra as uniaxial strain increases, using contours ε along the (a) p^ and (b) n^ directions. The inset in Fig. 14B shows selected dark-field spectra as strain increases. Fig. 14C shows peak scattering wavelength and Fig. 14D shows extracted linewidths, for strain in each direction. The dotted line in Fig. 14D shows yield strain. The inset in Fig. 14C shows reduction in scattering efficiency with strain. The inset in Fig. 14D shows movement of (111) plane spheres for different strain directions. The reader is referred to Fig. 3 of A. Kontogeorgos et al (2010) [A. Kontogeorgos, D.R.E. Snoswell, C.E. Finlayson, J.J. Baumberg, P. Spahn and G.P. Hellmann "Inducing Symmetry Breaking in Nanostructures: Anisotropic Stretch-Tuning Photonic Crystals, PRL 105, 233909 (2010)] which shows these drawings in colour, and the associated explanation of those drawings.

Tracking the darkfield scattering spectra (Fig. 14B inset) produces the maps in Figs. 14A and B as a function of strain for the p^ and n^ directions. The spectrum is dominated by the (111) Bragg peak for the fcc opal. For p^, only the single (111) scattering peak is observed, which blueshifts up to a strain of 50%. This contrasts to n^ for which the (111) peak blueshifts faster and additional features emerge. A short wavelength peak redshifts for ε >10%, and additional lower and higher energy peaks are observed for strains above

40% when the (111) peak disappears. It is noted that the model explained in relation to Fig. 15 below is a model for strains below 40%.

These induced anisotropies are more clearly seen by extracting the centre wavelength and linewidth of the Bragg peaks (see Figs. 14C and D). The $\varepsilon = 0$ fcc lattice is thus differently split by the action of strain in different directions. Below the yield strain of 20% (dashed line), the (111) plane Bragg wavelengths blueshift monotonically, at a rate almost double for n^ orientations (with $\frac{\Delta\lambda}{\lambda}$ = 61% per unit strain) than p^ ($\frac{\Delta\lambda}{\lambda}$ = 35% per unit strain). Similarly, the linewidth (which is a measure of the disorder in the opal) linearly increases by 20% for n^ while remaining unchanged for p^ . Above the yield strain, this anisotropy becomes extreme with the disappearance of the n^ (111) Bragg peak at $\varepsilon = 40\%$ when the red- and blueshifting peaks meet. Comparable anisotropy is seen in the Poisson's ratio v (see Fig. 13), which at low strains is 0.5 as expected for an fcc lattice, decreasing through the phase transition as the lattice deforms, except for an anomalously enhanced film thickness contraction seen in the n^ direction.

To understand this behaviour, consider a sphere packing model in which the initial fcc lattice undergoes a phase transition under applied strain into a monoclinic crystal lattice. This contrasts with the second-order phase transitions seen for hard-sphere atomic models of intermetallic compounds in which phase transformations in the crystal structure are induced by strain or temperature. Although the system here is physically 1000 times larger, it behaves similarly to predictions from atomic slip plane theory, providing a freely tunable analogue.

Fig. 15 shows a schematic hard-sphere model, showing how extension along [-101] (arrows along face of sample film) leads to shear along (-11-1) (arrows along plane inclined to face of sample film and solid arrows in inset), which pulls close-packed planes apart enough to allow slip (open arrow in inset).

Because of symmetry in this sample geometry (and supported by observations), the (111) plane (forming the upper and lower faces of the sample strips) of the initial fcc lattice deforms. Together with the maintenance of close packing, this model completely constrains the individual sphere motions. It is to be noted that the inventors present this model merely to assist in understanding of some embodiments of the invention and that the present invention is not necessarily bound by this theoretical model.

The reader is referred to Fig. 4b of A. Kontogeorgos et al (2010) which plots separation of (111) planes showing blueshifts of (111) for strain in the p^ and n^ directions. Free plane gliding occurs for 6% separation of close-packed planes (horizontal dashed line), which occurs for (-11-1) planes (inclined dashed line). Strength of diffraction is shown as the intensity of each point. The reader is referred to Fig. 4c of A. Kontogeorgos et al (2010) which shows the angle of reflection as measured from the normal to film surface as in Fig. 3.

Resolving the real-space and reciprocal-space lattices as strain is applied in different directions allows the plane spacings and orientations to be extracted (see Figs. 4b and 4c of A. Kontogeorgos et al (2010)). Immediately after the fcc lattice is deformed into the lower-symmetry monoclinic lattice, new normally forbidden Bragg peaks become visible (breaking the condition for fcc that h, k, and l must be all even or all odd). This new effect, which to the knowledge of the inventors has not been observed in atomic crystals, is the origin of the redshifting {211} planes seen only in the n^ direction. For larger strains the {110} planes also become visible at high angles, in complete contrast to the normal blueshifted colour effects. The model indeed predicts the appearance of redshifted previously forbidden planes (see Fig. 4c of A. Kontogeorgos et al (2010)), as well as the reduction in scattering strength of the (111) planes as strain is applied (see Fig. 14C, inset).

A further success of this simple model is the prediction of the yield strain. As is well known for the fcc lattice, linear strain produces glide in the {111} slip planes (see Fig. 15) which leads to plastic slip only when the close-packed sphere layers rise sufficiently over each other. The required increase in the (-11-1) slip plane spacing for a sphere sat in the triangular well between three touching spheres to move to the saddle between two of the spheres is $\sqrt{(9/8)} - 1 = 6\%$ expansion (see the horizontal dashed line, Fig. 4b of A. Kontogeorgos et al (2010)). The hard-sphere model predicts the expansion of this (-11-1) layer spacing for different stretch directions (inclined dashed lines in Fig. 4b of A. Kontogeorgos et al (2010)), exceeding the 6% critical threshold at strains of 20% for both p^ and n^ in good agreement with the data of Figs. 12 and 13. The yield stress should depend on the Schmidt factor for the different possible slip directions that can operate in the (-11-1) slip plane. This predicts 32% larger stress for the n^ direction (and hence

also the anisotropic Young's modulus), also in excellent agreement with the data in Figs. 12 and 13.

However, sphere packing does not predict the strong discontinuities observed for n^ in Figs. 14C and D around (and above) 40% strain, which indicate a second phase transition, possibly involving internal rearrangement of spheres within the structure to avoid sphere collisions. In addition, the model does not give a quantitative account of the elastic anisotropies observed in these photonic crystals. To progress beyond this simple model requires a full characterization of the microscopic elastomeric properties of the soft shell under both shear and compression. Experimentally, these properties can be modified by using alternative polymers with different molecular weights and methods of grafting onto the spheres and by subsequently modifying the cross-linking of the soft polymer matrix in which the hard spheres are embedded. The model thus fails when the independent hard sphere assumptions no longer hold, so that flow and rolling motion of individual spheres dominates for larger strains. However, most of the elastomeric opal film properties are indeed well reproduced by using the touching sphere assumption.

It is considered possible that further strain of the monoclinic lattice leads to a state, where again a fcc lattice is present. The new lattice is tilted compared to the original fcc lattice. This is important as the production of opal films in the melt tends always to lead to (111) parallel to the surface and therefore total reflection of other {111} planes (e.g. (-111) plane). Tilting the lattice by strain may therefore make these reflections visible.

In summary, these results provide strong evidence for the full 3D order of such polymer opals and demonstrate the ability of using uniaxial strain to generate structural phase transitions which break the lattice symmetry. The anisotropy observed along different axes of the polymer photonic crystal in both the elastic and optical properties is advantageously enhanced where there is a macroscopic single domain over the whole sample and induces new optical scattering phenomena.

Experimental

Preparation of monodisperse Core-Interlayer-Shell polymer beads

The beads produced here were similar to those described in US 2004/0253443.

A 10 L reactor with stirrer, condenser, argon inlet and heating mantle was heated to 75°C and flushed with argon.

2.750 g sodium dodecylsulfate
2800.000g demineralised water
36.000g styrene
4.000g butane dioldiacrylate

were premixed and fed into the reactor. The stirrer was adjusted to 250 rpm. The temperature of the mixture was monitored. At 65°C, three freshly prepared solutions were subsequently added:

0.360g sodium disulfite in 5g demineralised water
5.180g sodium persulfate in 20 g demineralised water
0.360g sodium disulfite in 5g demineralised water

Cloudiness was observed after 10 min. After an additional 10 min, an emulsion consisting of

2.300g sodium dodecylsulfate
4.000g potassium hydroxide
2.200g Dowfax2A1
900.000g demineralised water
700.000g styrene
70.000g butane dioldiacrylate

was fed dropwise at 10 mL/min. 30 min after the addition was finished, a freshly prepared solution of

0.250g sodium persulfate in 5 g demineralised water

was added. After 15 min, a second emulsion consisting of

0.500g sodium dodecylsulfate

2.100g Dowfax 2A1
320.000g demineralised water
250.000g methyl methacrylate
30.000g allyl methacrylate

was fed dropwise at 14 mL/min. 20 min after the addition was finished, a third emulsion consisting of

4.000g sodium dodecylsulfate
2.000g potassium hydroxide
1600.000g demineralised water
1400.000g ethylacrylate

was added dropwise at 18 mL/min. The synthesis was terminated 60 min after the last addition was finished. The latex was filtered through a 100µm sieve and added dropwise into a mixture of 17 L methanol and 100mL of concentrated aqueous solution of sodium chloride under stirring. The polymer coagulated and formed a precipitate which settled after the stirring was terminated. The clear supernant was decanted, the precipitate was mixed with 5 L demineralised water and subsequently filtered through a 100micron sieve. The filter cake was dried for three days at 45°C in a convective oven.

Preparation of monodisperse Core-Interlayer-Shell polymer beads with higher Tg

A 10 L reactor with stirrer, condenser, argon inlet and heating mantle was heated to 75°C and flushed with argon.

2.750 g sodium dodecylsulfate
2800.000g demineralised water
36.000g styrene
4.000g butane dioldiacrylate

were premixed and fed into the reactor. The stirrer was adjusted to 250 rpm. The temperature of the mixture was monitored. At 65°C, three freshly prepared solutions were subsequently added:

0.360g sodium disulfite in 5g demineralised water,
5.180g sodium persulfate in 20 g demineralised water
0.360g sodium disulfite in 5g demineralised water

Cloudiness was observed after 10 min. After an additional 10 min, an emulsion consisting of

2.300g sodium dodecylsulfate
4.000g potassium hydroxide
2.200g Dowfax2A1
900.000g demineralised water
700.000g styrene
70.000g butane dioldiacrylate

was fed dropwise at 10 mL/min. 30 min after the addition was finished, a freshly prepared solution of

0.250g sodium persulfate in 5 g demineralised water

was added. After 15 min, a second emulsion consisting of

0.500g sodium dodecylsulfate
2.100g Dowfax 2A1
320.000g demineralised water
250.000g ethylacrylate
30.000g allyl methacrylate

was fed dropwise at 14 mL/min. 20 min after the addition was finished, a third emulsion consisting of

4.000g sodium dodecylsulfate
2.000g potassium hydroxide
1600.000g demineralised water
404.7g ethylacrylate
603.3g isobutyl methacrylate

42g hydroxyethyl methacrylate

was added dropwise at 18 mL/min. The synthesis was terminated 60 min after the last addition was finished. The latex was filtered through a 100µm sieve and added dropwise into a mixture of 17 L methanol and 100mL of concentrated aqueous solution of sodium chloride under stirring. The polymer coagulated and formed a precipitate which settled after the stirring was terminated. The clear supernant was decanted, the precipitate was mixed with 5 L demineralised water and subsequently filtered through a 100micron sieve. The filter cake was dried for three days at 45°C in a convective oven.

Preparation of monodisperse Core-Interlayer-Shell polymer beads with chemical functionality for the crosslinking with polyisocyanates

A 10 L reactor with stirrer, condenser, argon inlet and heating mantle was heated to 75°C and flushed with argon.

2.750 g sodium dodecylsulfate
2800.000g demineralised water
36.000g styrene
4.000g butane dioldiacrylate

were premixed and fed into the reactor. The stirrer was adjusted to 250 rpm. The temperature of the mixture was monitored. At 65°C, three freshly prepared solutions were subsequently added:

0.360g sodium disulfite in 5g demineralised water
5.180g sodium persulfate in 20 g demineralised water
0.360g sodium disulfite in 5g demineralised water

Cloudiness was observed after 10 min. After additional 10 min, an emulsion consisting of

2.300g sodium dodecylsulfate
4.000g potassium hydroxide
2.200g Dowfax2A1
900.000g demineralised water

700.000g styrene
70.000g butane dioldiacrylate

was fed dropwise at 10 mL/min. 30 min after the addition was finished, a freshly prepared solution of

0.250g sodium persulfate in 5 g demineralised water

was added. After 15 min, a second emulsion consisting of

0.500g sodium dodecylsulfate
2.100g Dowfax 2A1
320.000g demineralised water
250.000g ethylacrylate
30.000g allyl methacrylate

was fed dropwise at 14 mL/min. 20 min after the addition was finished, a third emulsion consisting of

4.000g sodium dodecylsulfate
2.000g potassium hydroxide
1600.000g demineralised water
1358.000g ethylacrylate
42g hydroxyethylmethacrylate

was added dropwise at 18 mL/min. The synthesis was terminated 60 min after the last addition was finished. The latex was filtered through a 100µm sieve and added dropwise into a mixture of 17 L methanol and 100mL of concentrated aqueous solution of sodium chloride under stirring. The polymer coagulated and formed a precipitate which settled after the stirring was terminated. The clear supernant was decanted, the precipitate was mixed with 5 L demineralised water and subsequently filtered through a 100micron sieve. The filter cake was dried for three days at 45°C in a convective oven.

Preparation of polymer compounds with additives for the melt-processing

100 g of polymer was mixed with 1 g of Licolub FA1 (Clariant) and 0.05 g Special Black 4 (Evonik) at 140°C and 100 rpm in an twin-screw DSM Xplore µ5 microextruder. The material was passed 4 times through the extruder.

Preparation of a compound of CS354 for the melt processing with a polyisocyanate crosslinker

100 g of polymer was mixed with 1% Licolub FA1 (Clariant), 3% Crelan UI (BayerMaterialScience) and 0.05 g Special Black 4 (Evonik) in an twin-screw DSM Xplore µ5 microextruder at 120°C and 100 rpm. The material was passed 4 times through the extruder.

Preparation of a compound of CS330 for the melt processing with photoinitiator for additional photocrosslinking

100 g of polymer was mixed with 1% Licolub FA1 (Clariant), 2% benzophenone (Sigma-Aldrich) and 0.05g Special Black 4 (Evonik) in an twin-screw DSM Xplore µ5 microextruder at 120°C and 100 rpm. The material was passed 4 times through the extruder.

Preparation of opal disks by pressing

6 g of polymer compound was heated on a hotplate set to 150°C. The softened polymer mass was placed between two PET foils and two polished, high-gloss ironless steel sheets and pressed in a Collin press at 150°C and 130 bar hydraulic pressure for 3 minutes.

****

The embodiments set out above have been described by way of example. On reading this disclosure, modifications of these embodiments, further embodiments and modifications thereof will be apparent to the skilled person and as such are within the scope of the present invention.

CLAIMS

1. A composite optical material having a three dimensional arrangement of core particles distributed in a matrix, the refractive index of the material of the core particles being different to the refractive index of the material of the matrix and the three dimensional arrangement having a periodicity such that, when a surface of the material is illuminated with white light, the composite material exhibits structural colour, wherein the three dimensional periodic arrangement is a reduced symmetry arrangement based on a crystallographic close-packed arrangement but strained therefrom to have reduced symmetry about a rotational axis perpendicular to the surface compared with the crystallographic close-packed arrangement so that Bragg reflections from planes disposed at oblique angles to the surface that would be forbidden in the crystallographic close-packed arrangement or would be subject to total internal reflection at the surface are allowed and visible from the reduced symmetry arrangement, thereby providing a variation in intensity and/or wavelength of structural colour with rotation of the material about an axis perpendicular to the surface when viewed obliquely while the viewing angle remains substantially constant.

2. A composite optical material according to claim 1 wherein when sufficiently deformed, the material preferably mechanically fails before the strain of the deformation is sufficient to force the reduced symmetry arrangement to return to the crystallographic close-packed arrangement.

3. A composite optical material according to claim 1 or claim 2 wherein the core particles are disposed in the composite material in an arrangement based on a face centred cubic lattice.

4. A composite optical material according to any one of claims 1 to 3 wherein the crystallographic structure of the reduced symmetry arrangement is selected from: a monoclinic structure; and a tilted fcc structure.

5. A method for manufacturing a composite optical material, the method including the steps:

in a first configuration of the composite optical material, providing a crystallographic close-packed arrangement of core particles distributed in a matrix,

the refractive index of the material of the core particles being different to the refractive index of the material of the matrix and the arrangement having a periodicity such that, when a surface of the material is illuminated, the arrangement exhibits Bragg reflection, optionally in the visible spectrum, the crystallographic close-packed arrangement having a degree of symmetry such that Bragg reflections from at least one set of crystallographic planes are forbidden or are subject to total internal reflection at the surface;

transforming the first configuration of the composite optical material to a second configuration by straining the crystallographic close-packed arrangement to provide a reduced symmetry arrangement having reduced symmetry about a rotational axis perpendicular to the surface compared with the crystallographic close-packed arrangement so that Bragg reflections from planes disposed at oblique angles to the surface that were forbidden in the crystallographic close-packed arrangement or subject to total reflection at the surface are allowed and visible from the reduced symmetry arrangement.

6. A method according to claim 5 wherein the method further includes the step of treating the composite optical material in order to constrain the material in the second configuration from returning to first configuration.

7. A method according to claim 6 wherein the matrix material is treated by cross-linking treatment.

8. A method according to claim 6 wherein the matrix material is treated to raise Tg of the matrix material.

9. A method according to claim 6 wherein the matrix is in the first configuration above Tg of the matrix material, and then cooled to below Tg in the second configuration.

10. A method according to claim 6 wherein the composite optical material is permanently bonded to a support, in order to hold the matrix material and thus prevent return of the second configuration to the first configuration.

11. A method according to any one of claims 5 to 10 wherein the step of transforming the first configuration of the composite optical material to the second configuration

includes the step of straining the crystallographic close-packed arrangement along a direction that is not parallel to a close packed direction in the crystallographic close-packed arrangement.

12. A method according to any one of claims 5 to 11 wherein the step of transforming the first configuration of the composite optical material to the second configuration includes the step of straining the crystallographic close-packed arrangement along a direction that is substantially perpendicular to a close packed direction in the crystallographic close-packed arrangement.

13. A method according to any one of claims 5 to 12 wherein the strain applied to the composite optical material is tensile strain.

14. A method according to any one of claims 5 to 13 wherein the strain applied during the step of transformation from the first configuration to the second configuration is at least 40%.

15. A method according to any one of claims 5 to 14 wherein the composite optical material is formed by shear processing of a precursor composite material in a shear processing direction, and the strain applied during the step of transformation from the first configuration to the second configuration is not parallel to the shear processing direction.

16. A method according to any one of claims 5 to 15 wherein the composite optical material is formed by shear processing of a precursor composite material in a shear processing direction, and the strain applied during the step of transformation from the first configuration to the second configuration is substantially perpendicular to the shear processing direction.

17. A method according to any one of claims 5 to 16 wherein the crystallographic structure of the composite optical material in the second configuration is a monoclinic structure.

18. A composite optical material obtained by, or obtainable by, a method according to any one of claims 5 to 17.

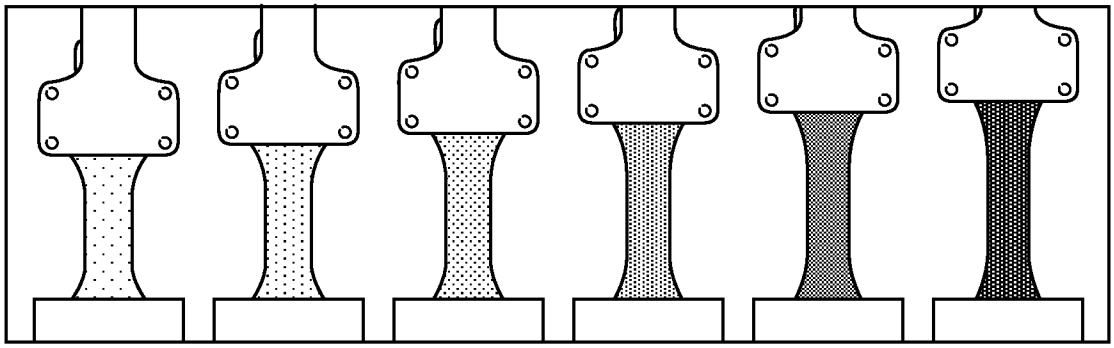

FIG. 1

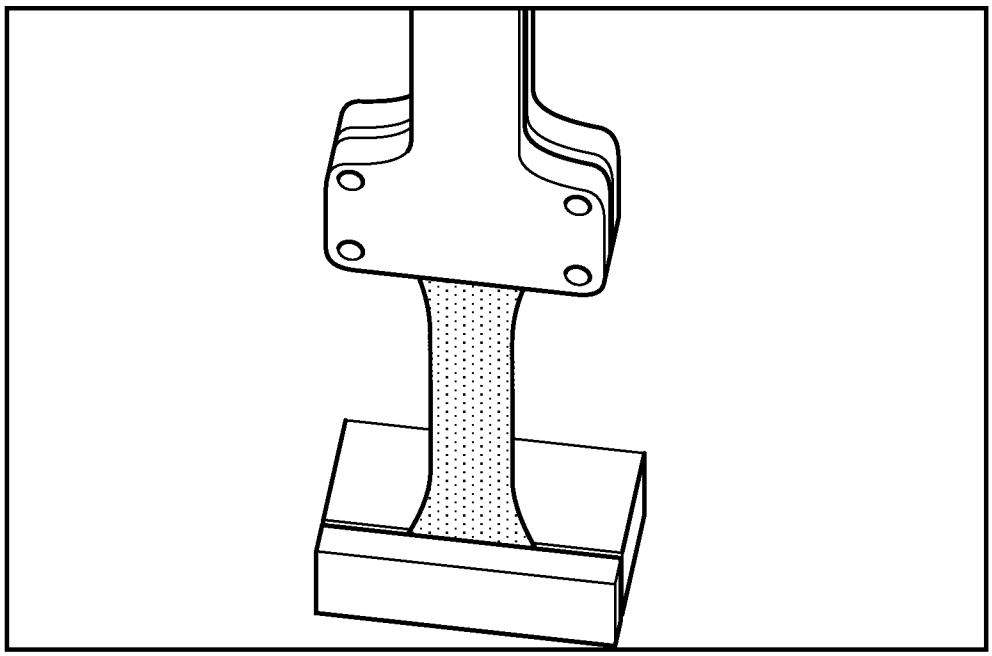

FIG. 2

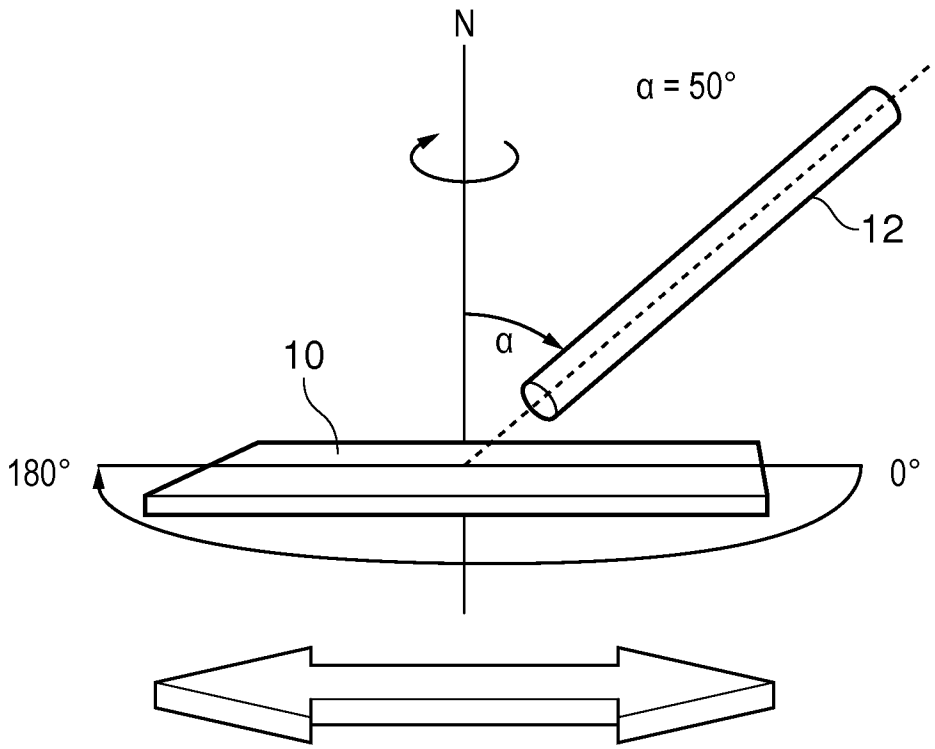

FIG. 3

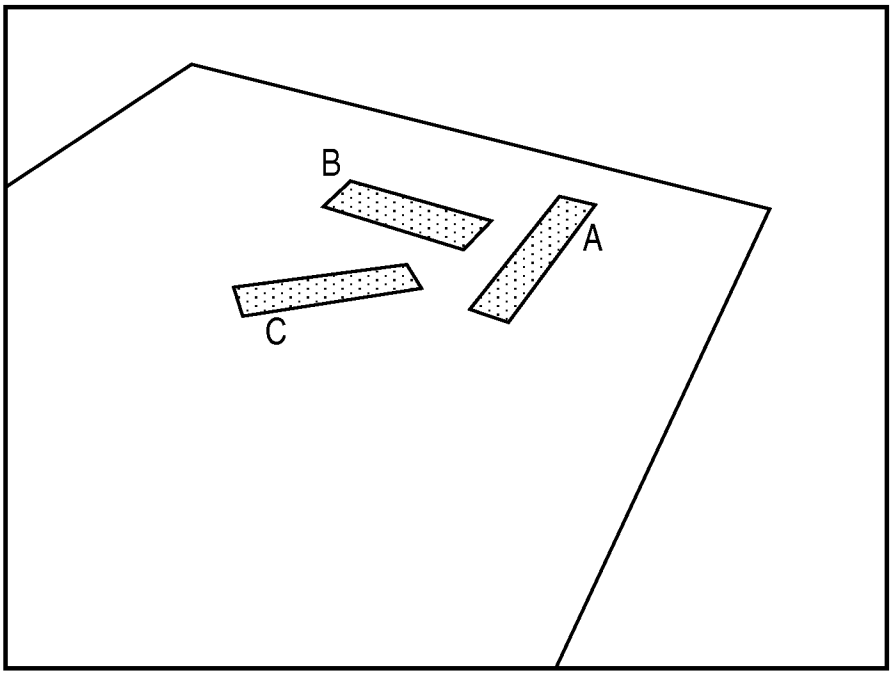

FIG. 4

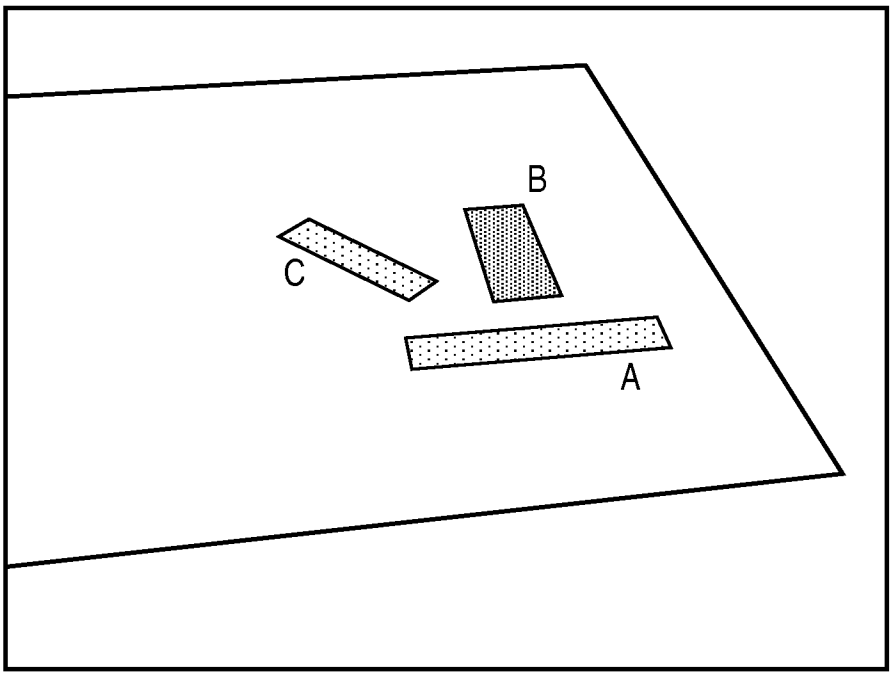

FIG. 5

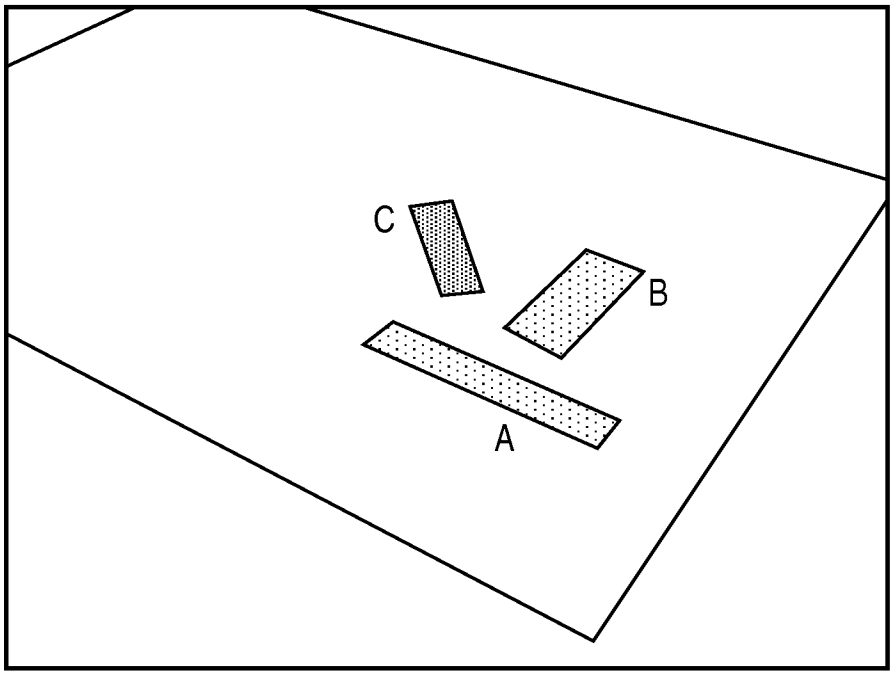

FIG. 6

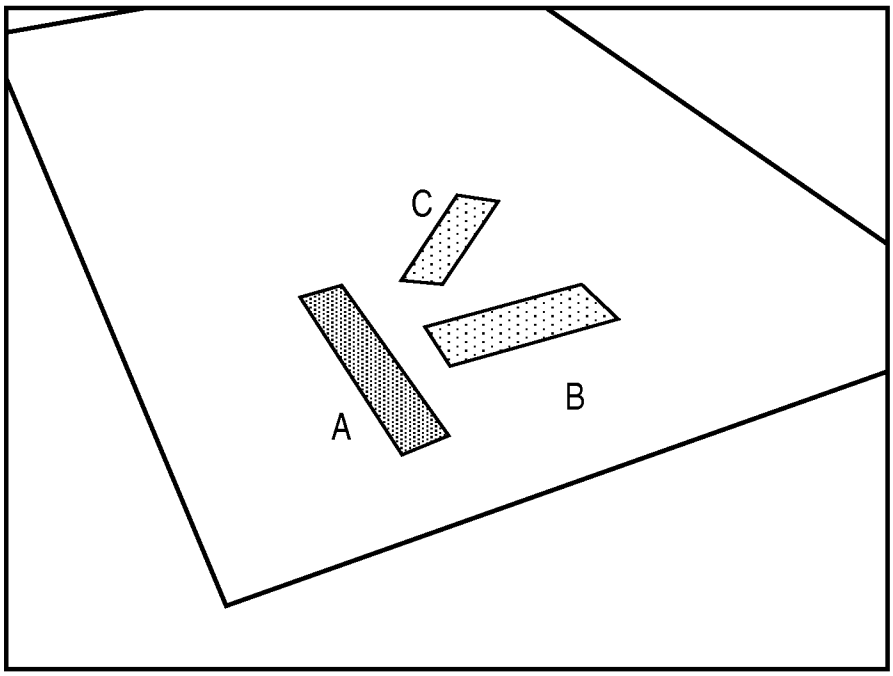

FIG. 7

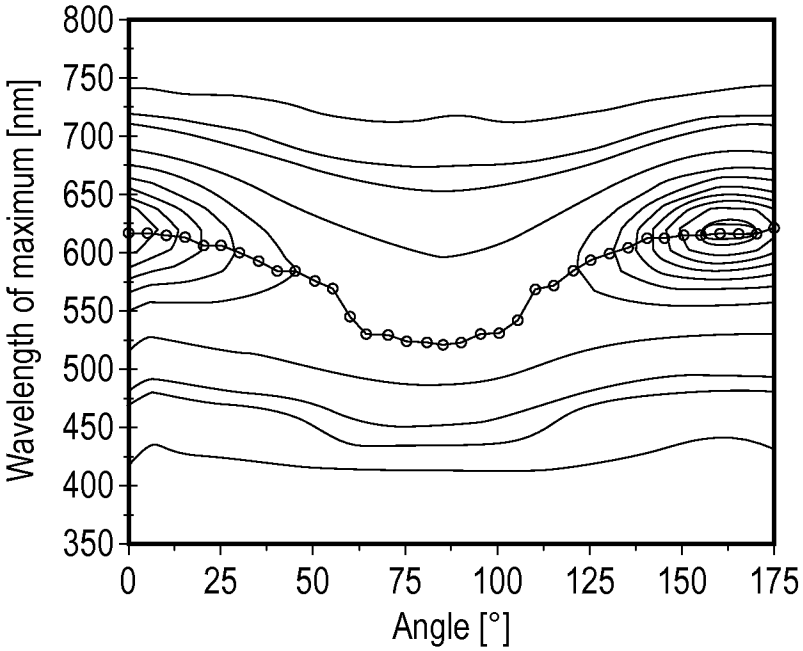

FIG. 8A

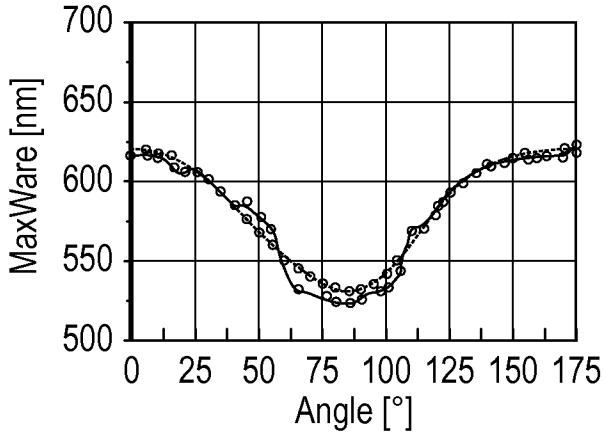

FIG. 9A

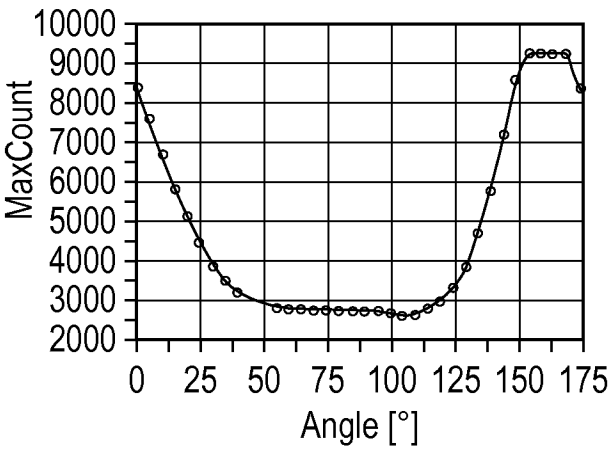

FIG. 10A

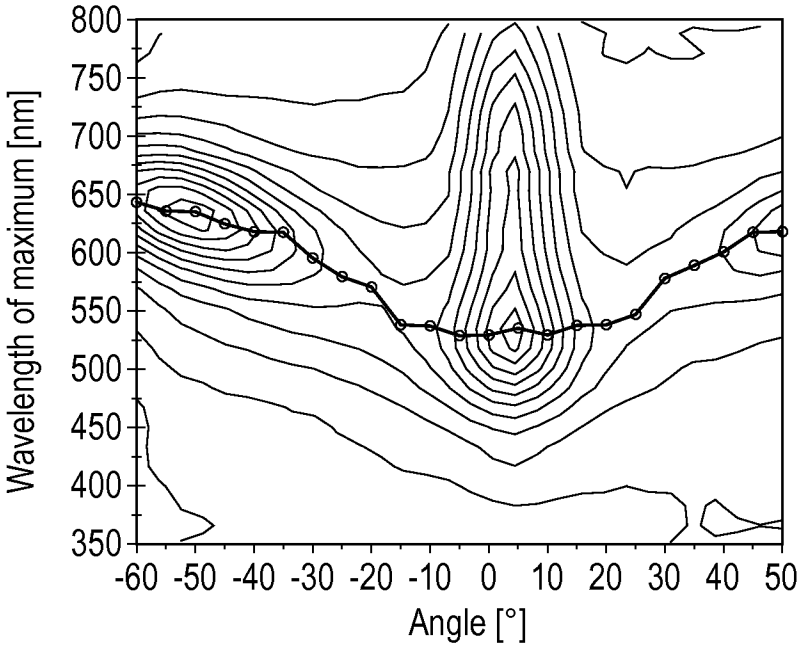

FIG. 8B

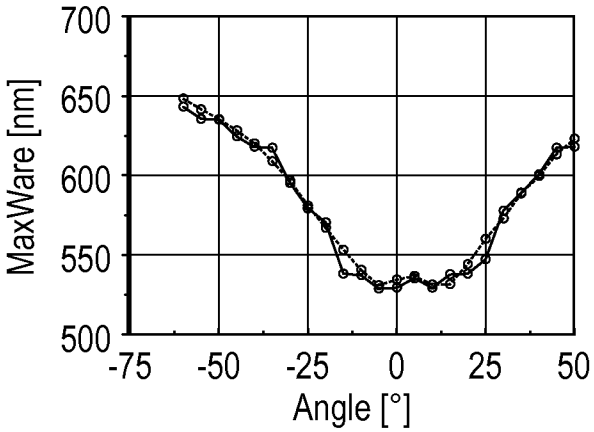

FIG. 9B

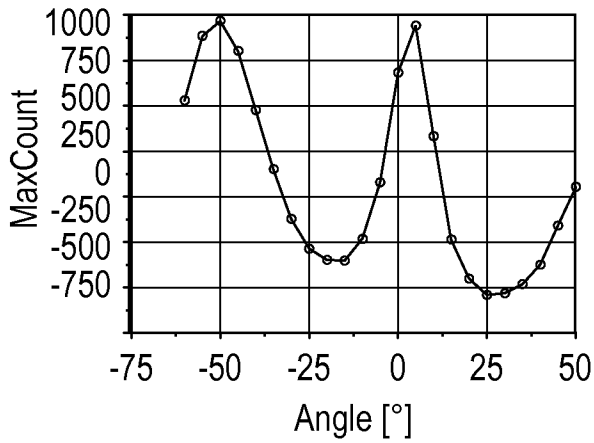

FIG. 10B

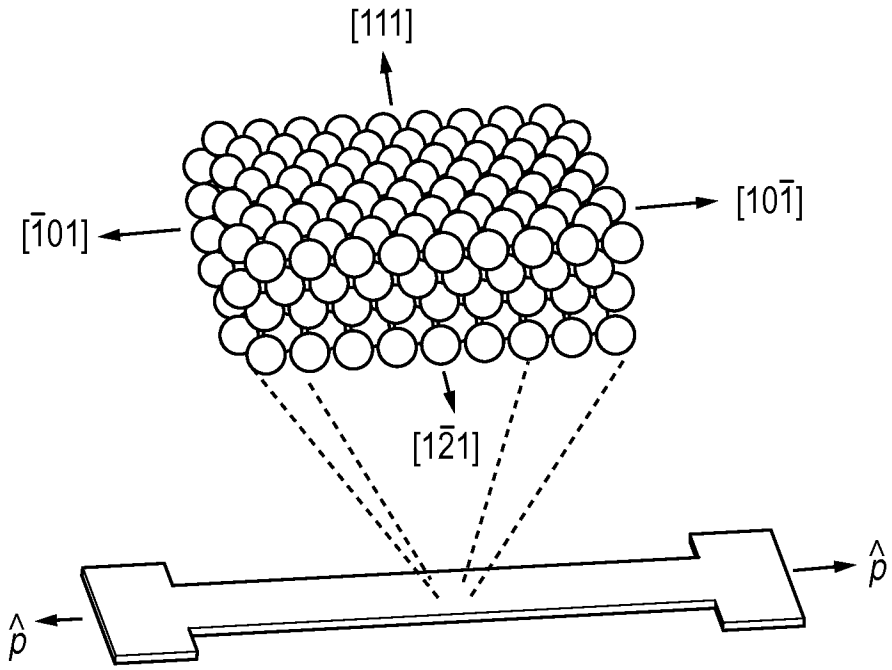

FIG. 11A

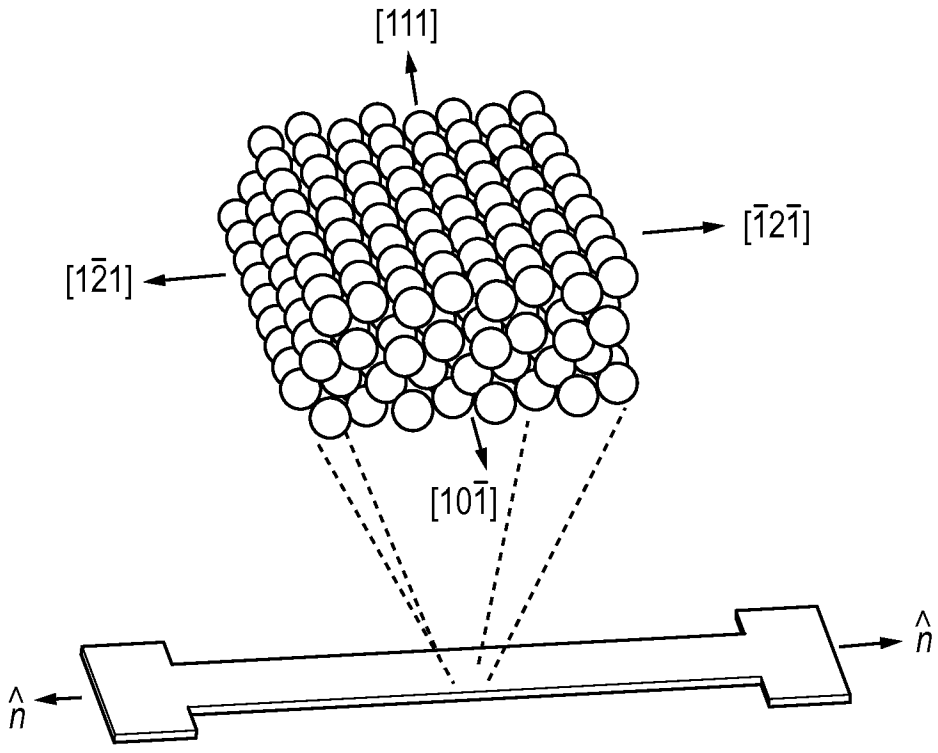

FIG. 11B

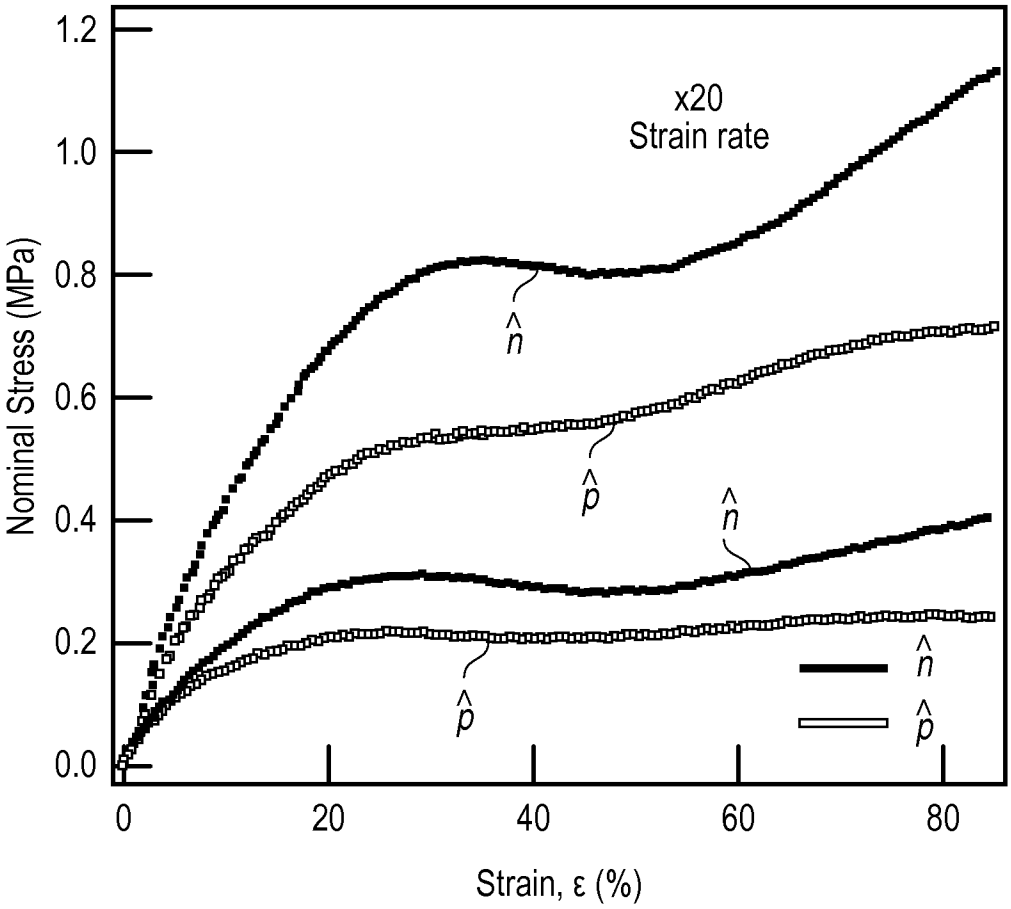
1.2
1.0
0.8
0.6
0.4
0.2
0.0
Nominal Stress (MPa)
x20
Strain rate
n̂
p̂
n̂
p̂
n̂
p̂
0
20
40
60
80
Strain, ε (%)

FIG. 12

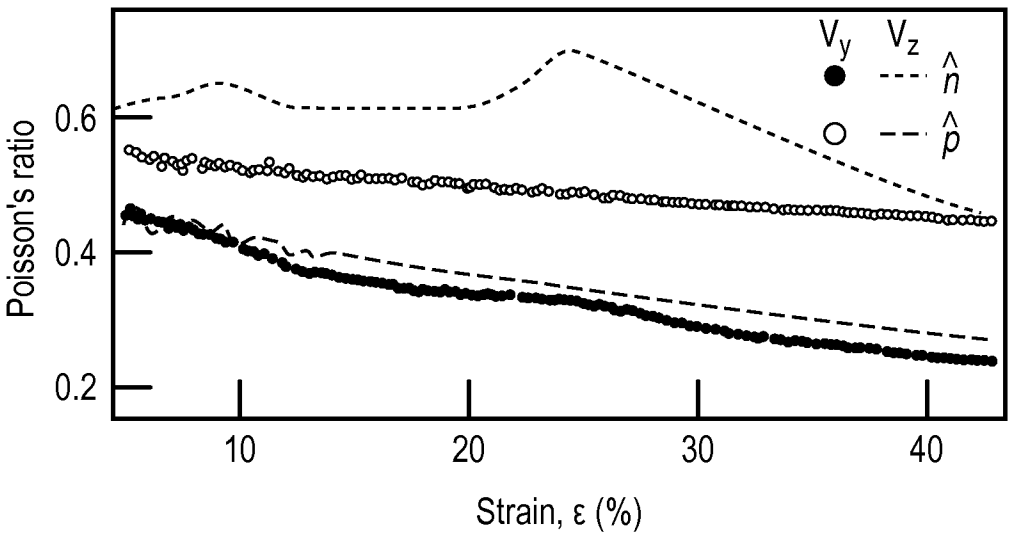
0.6
0.4
0.2
Poisson's ratio
Vy
Vz
n̂
p̂
10
20
30
40
Strain, ε (%)

FIG. 13

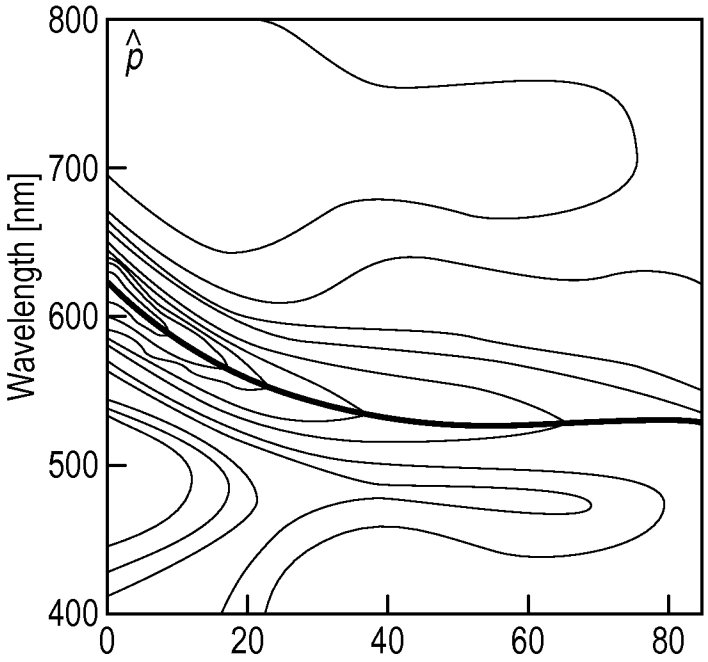

FIG. 14A

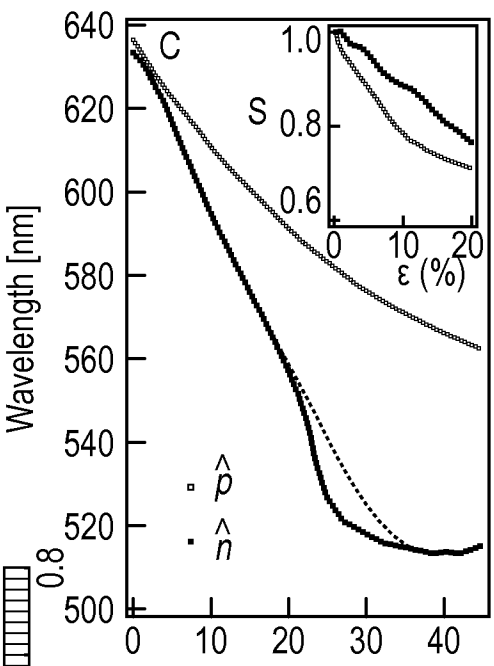

FIG. 14C

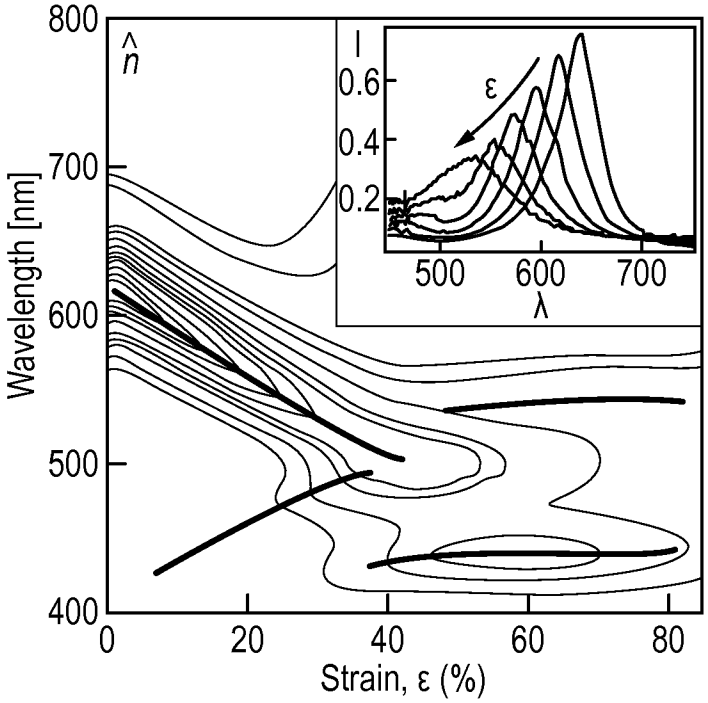

FIG. 14B

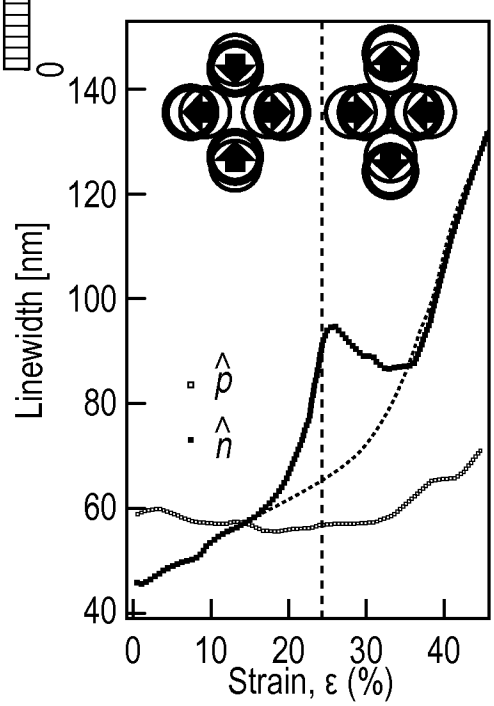

FIG. 14D

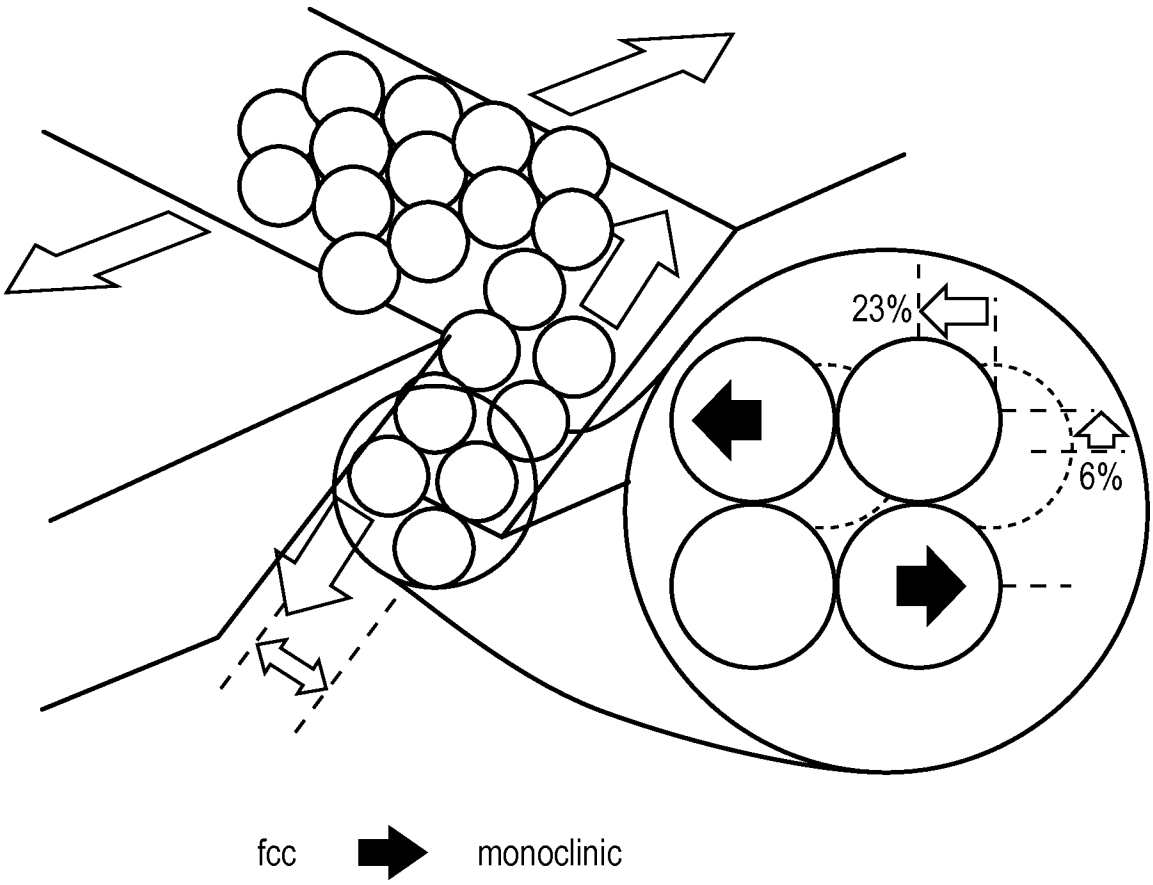

FIG. 15